NASA Contractor Report 198473

# Structural Analysis and Properties of Impact Ices Accreted on Aircraft Structures

R.J. Scavuzzo, M.L. Chu, and C.J. Kellackey
*University of Akron*
*Akron, Ohio*

April 1996

Prepared for
Lewis Research Center
Under Grant NAG3–479


National Aeronautics and
Space Administration

## Table of Contents

List of Figures

**ABSTRACT**

This final contractor report presents a summary of work done on the experimental measurements of the mechanical properties of impact ices and analytical studies of ice stresses and mechanical deicing systems. Experimental work on the adhesive shear strength, the peel strength, the bending strength and tensile strength of impact ices.

The major analytical studies that were completed are as follows:

(1) Ice shedding by the EIDI system
(2) Impact Ice stresses in rotating airfoils
(3) Aerodynamic forces in ice shedding
(4) Interface shear stresses from bending and twisting
(5) Statistical structural analysis of ice shedding from rotating airfoils.

In this report, results and data from each experimental and analytical study are summarized. A total of twenty (20) technical papers and one MS Thesis were written and/or presented from the work done in this project.

## 1.0 INTRODUCTION

Impact ice formations on airfoils, jet engine inlets, propellers or helicopter blades adversely affect the safety of aircraft. As a result, NASA LRC has a continuing research program which covers many different icing problems. New regulations and procedures are continually instituted by the FAA to improve aircraft safety as a result of contributions of this research.

The overall objective of this project is to develop methods to predict the mechanical shedding of impact ice adhered to airfoil surfaces or to propellers and helicopter blades. At the initiation of this project there was very little data on the insitu mechanical properties of impact ice. Therefore, a significant effort was made to measure various mechanical properties of impact ice and to use these properties in mechanical analyses. Analytical methods, primarily based on finite element analyses, were developed to predict shedding of impact ice from various surfaces caused by inertia forces or aerodynamic forces.

Two major experimental programs were conducted: one to measure the adhesive shear strength of impact ice adhered to aluminum, stainless steel, neoprene rubber and titanium and, two, to measure the tensile strength of impact ice. In addition, an effort was made to measure the peel strength of impact ice adhered to various surfaces and to evaluate the bending failures of ice adhered to aluminum.

The major analytical studies that were completed are as follows:

(1) Ice shedding by the EIDI system
(2) Impact Ice stresses in rotating airfoils
(3) Aerodynamic forces in ice shedding
(4) Interface shear stresses from bending and twisting
(5) Statistical structural analysis of ice shedding from rotating airfoils.

In this report, results and data from each experimental and analytical study are summarized. A total of twenty (20) technical papers [1-20] and one MS Thesis [21] were written and/or presented from the work done in this project. Six of the twenty papers are refereed journal publications. A list of these publications is provided in Section 6.0. Directions for additional research to determine needed mechanical properties of impact ice and analytical work are suggested.

## 2.0 EXPERIMENTAL WORK

### 2.1 Shear Stress Data

Shear stress data were gathered during a series of tests conducted inside NASA-Lewis Icing Research Tunnel (IRT) facilities using test apparatus, which is shown in the schematic

diagrams of Figures 1 and 2. The two main sections of the equipment used were: (1) the ice forming section where impact ices were accreted on the test specimens, and (2) the test section where the adhesive shear force was measured. The test specimen consisted of a thin outer cylinder with a window and end flanges and a hollow inner cylinder. Five of the cylinder pairs were stacked on top of each other on a common shaft which was mounted vertically in the IRT. The assembly was usually rotated in the wind tunnel at a rate of about 20 rpm. When the stack was rotated, an almost uniform coating of ice was deposited on the cylinders. In a few tests, the window was aligned up stream and the stack was not rotated. Under this condition, ice formed over the window and adjacent area only. Two types of windows were used: a square window and a rectangular window. Time of exposure to the ice cloud was varied so that the thickness of the ice deposit was approximately 1/4" to 3/8" thick. It was found that if the ice was too thin, cohesive failure would occur in the window section. As expected, this type of failure occurred more often with rime ice than with glaze ice. Furthermore, the rime ice accreted with small water drops (15 microns) appeared to be weaker than that developed with larger drops (20-27 microns). On the other hand, if the ice was too thick, the stack assembly could not be taken apart without significant force, which often disturbed the adhesive bond between the inner cylinder and ice. By trial and error it was found that the optimum thickness for testing was about 1/4" for glaze ice and about 3/8" for rime ice. Another aspect about testing rime ice should be pointed out. Bumps and depressions in the surface of the specimen affected the shape of the ice deposit. Thus, the lip at the window edge of the outer cylinder could be easily distinguished in a 3/8" ice deposit even though the lip was filed to a sharp edge. This problem was worse with small drops (15 microns) and at low temperatures ($-8^0$ F). This weakness in rime ice often lead to a cohesive failure along the window edges rather than an adhesive failure on the surface of the inner cylinder. None of this cohesive failure data was used. Also, it should be mentioned, as is inherent with icing research, there was a large amount of scatter in the data.

### 2.1.1 Trends

Parametric experimental studies revealed that the adhesive shear strength of accreted impact ice is statistically independent of the following: tunnel air temperature below 4 degrees C ($25^\circ$ F); the thickness of accreted ice (testing showed no difference for thicknesses varying between 1/16" and 1/2"); the metal substrate material; different window shapes (rectangular versus square); the cloud on or cloud off testing condition; and the ice accretion shape (uniform versus non-uniform).

Three parameters examined in the study, however, did have correlative effects with the adhesive shear strength: wind

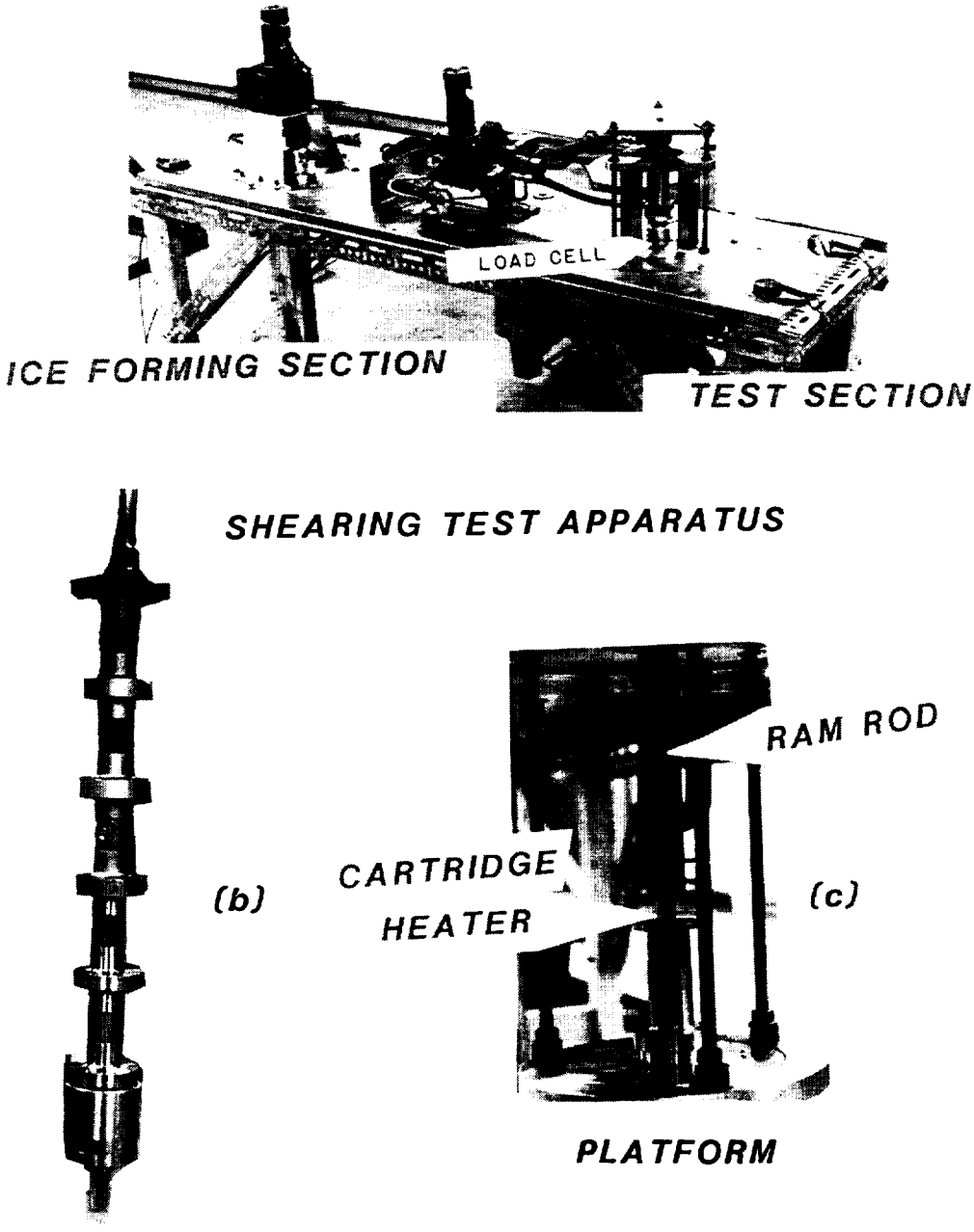


Figure 1 NASA Shear Test Apparatus

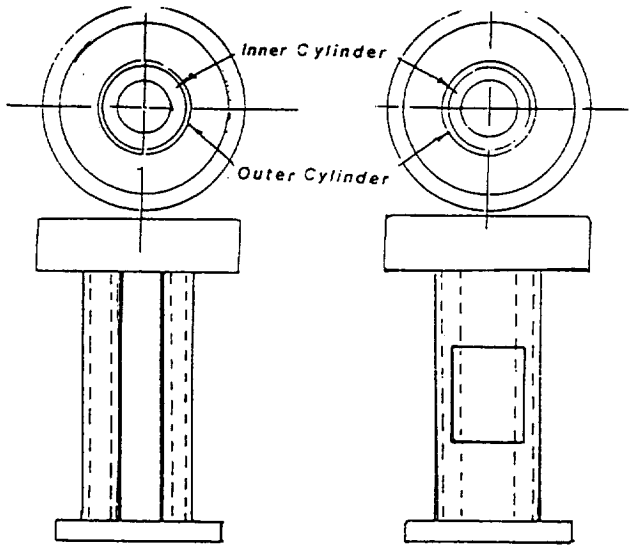


Figure 2 Shear Test Specimens

velocity, drop size and ice surface temperature. Adhesive shear strength is dependent upon wind velocity for both hard rime and glaze ice deposits. For hard rime-glaze ice, the adhesive shear strength appeared to increase slightly as the wind velocity and drop size increase. However, for powdery rime ice (-8° F to 3° F), there appeared to be no discernible trend at all. In the majority of the test samples with these particular conditions, the ice deposits at the window shattered during the shearing test; therefore, the statistical conclusions are not reliable due to limited statistical points. From statistical plots, it can be seen that the shear strength increased slightly with increasing droplet momentum [4,21].

### 2.1.2 Shear Stress Versus Temperature

A thermocouple embedded in the center of the inner cylinder wall near the center of the rectangular window was used to measure cylinder temperature as the specimen was being heated by a cartridge heater. A finite element transient heat conduction calculation was made using NASTRAN, which accounted for the ice layer, stainless steel housing and inner metal cylinder. It was determined from this analysis that the difference in temperature between the ice interface and point of measurement was less than about 1° F. When the heater was turned on, the temperature on the cylinder rose slowly. From 5 to 10 minutes was needed to reach a predetermined cylinder temperature. The instant that the predetermined temperature was attained, the hydraulic cylinder was actuated to shear the specimen. In this manner, shear stress as a function of temperature was determined.

There appears to be a strong correlation between the ice-substrate interface temperature and the adhesive shear strength. At an interface temperature above 25° F, the shear strength, on the average, tended to decrease and approaches zero at the melting point temperature of 32° F. This trend can be seen in Figure 3.

### 2.1.3 Best Statistical Fit

Since impact adhesive and tensile properties of impact ices are somewhat random in nature, a statistical averaging approach was used to predict the probability of shedding of impact ices from a rotating rotor blade.

The first task of this approach is to analyze statistically the adhesive shear strength data previously collected by Scavuzzo and Chu [2,4,13]. This analysis includes predicting the characteristics of the data (namely, the most probable average shear strength and its distribution) from the limited sample of data collected. This data were divided into 15 groups in which the wind speed and droplet size (the two dependent variables of shear strength) were held constant. Then several cumulative failure distributions were tried in fitting the data. The five different distribution types considered were: the Weibull distribution; the two-parameter Weibull distribution; the exponential distribution; the Gumbel distribution of the smallest extreme; and the Gumbel distribution of the largest extreme. These distributions were chosen because material failure follow closely these distributions, particularly the Weibull distribution.

To determine which distribution best describes the data, the nonlinear equations of the fine cumulative distribution functions were transformed into a linear form. The shear stress data are then fitted to these linear forms to determine which distribution has the best fit. With the least squares line and its parameters established, a measure of the best fit is determined by calculating the correlation coefficient, R. Then the fifteen groups of data were plotted using the straight line fits, and the distribution's parameters computed. Correlation coefficients were then compared. Figure 4 shows a typical linear fit of data points. It appeared that both Weibull and Gumbel Distributions with large extreme best describes the variations in the shear strength data, but for simplicity the Weibull distribution was chosen.

## 2.2 Peel Test Results

Two test programs to determine the peel strength of ice were conducted: one program on impact ice in the IRT [4, 20] and one program in a laboratory at the University of Akron [6].

Impact ice peeling strength was measured in the IRT in the following manner. A rotating cylindrical aluminum drum

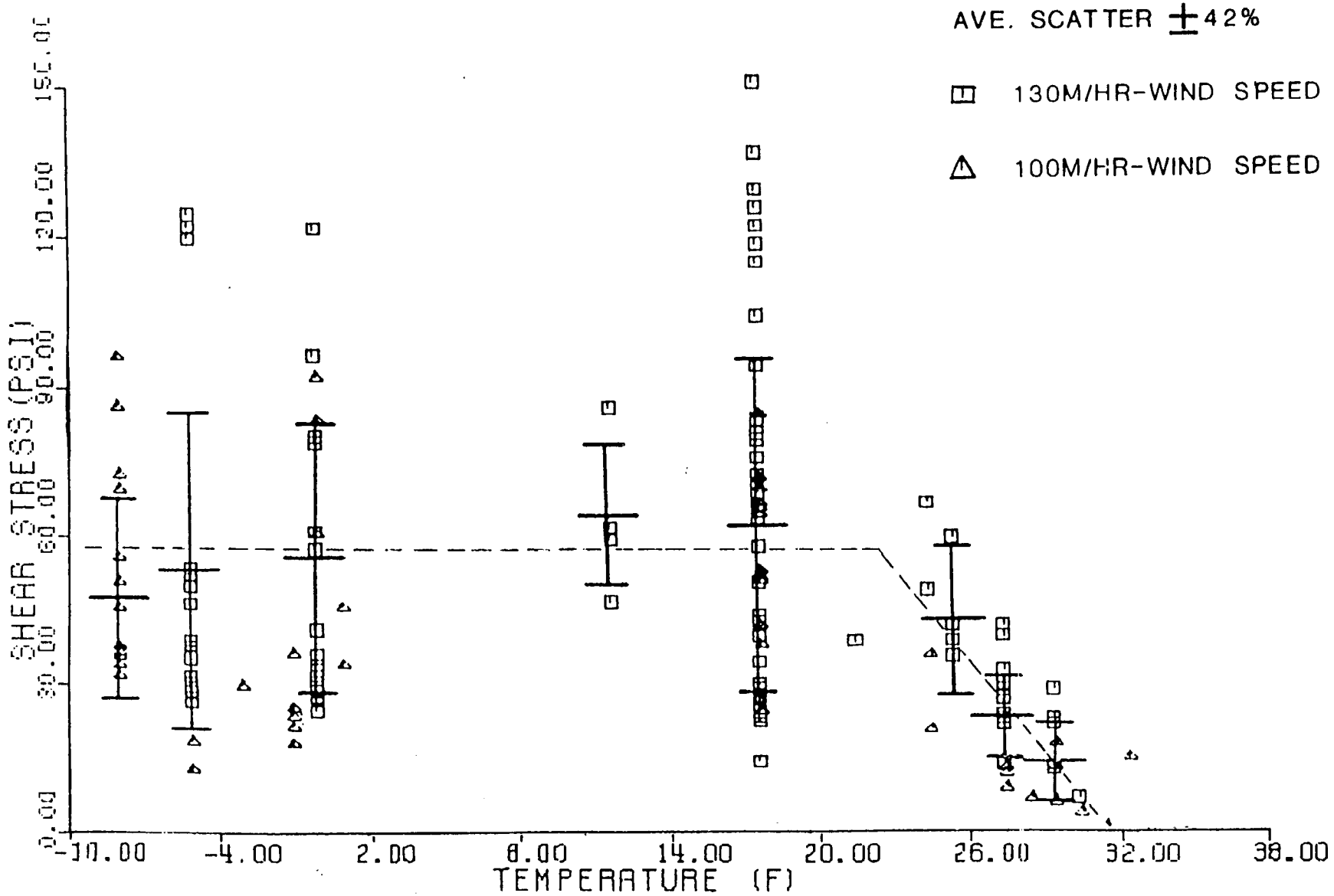


Figure 3 Adhesive Shear Strength Data as a Function of Temperature

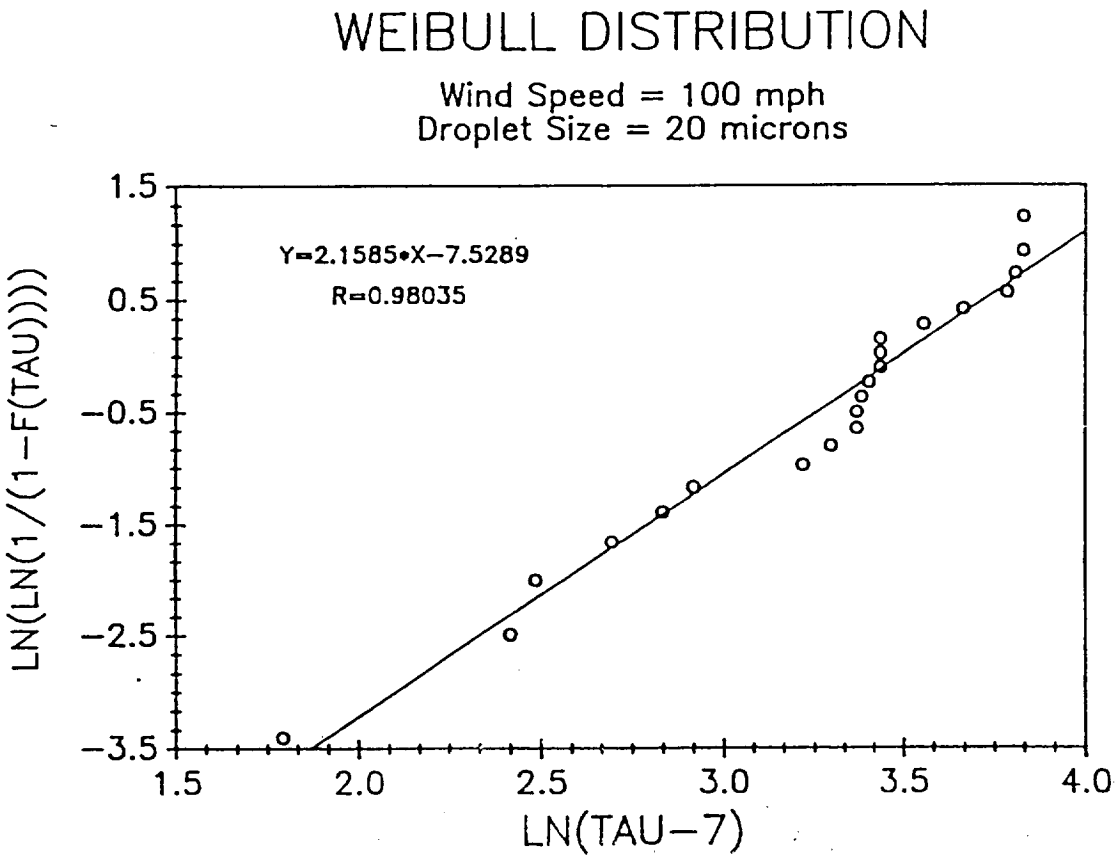


Figure 4 Straight Line Log Fit of Shear Strength Data to a Weibull Distribution (Wind Speed = 100 mph, 20 Micron Drop)

apparatus was designed and constructed with window slots for thin rectangular specimens of different materials that were held flush to the surface of the cylinder (Figure 5). The cylinder was either rotated or held in a fixed position with a specimen up stream in order to build up an ice coating. Specimen strips were peeled from the ice with a thin stainless steel wire through a load cell to measure the peeling force. The angle of peel could be varied by adjusting the height of the yoke relative to the bottom of the specimen. Peel angles ranged from 20 to 90 degrees. Three specimen types were used in this test: aluminum, 316 stainless steel .003" shim stock and a neoprene faced composite. Testing showed that the peeling stress (force/unit width) differed with substrate material. As seen in Figure 6, the peeling stress for the neoprene composite tends to be higher than for the metal stripes. However, all these values are low, varying between 2 and 4.8 lb/in. There was no significant increases in peel strength as the peel angle increased. A few tests were performed manually at 0 angle of peel. This test was equivalent to the shear strength test. For these cases, a large adhesive shear strength was obtained. The peel strength between 0 and 20 degrees could not be investigated with the current apparatus. Further testing in the IRT is needed to examine this region since pneumatic and EIDI de-icers

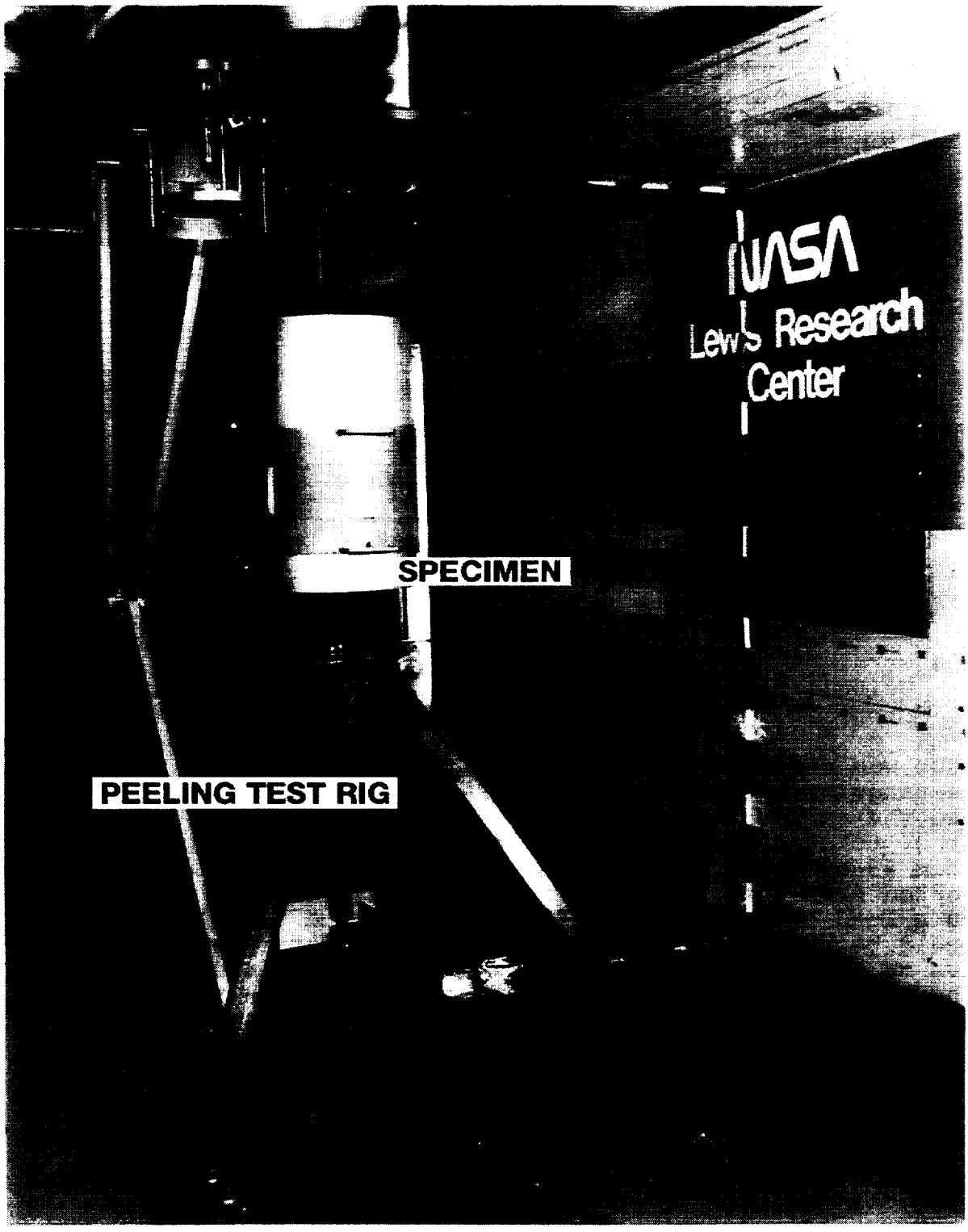


Figure 5 IRT Peel Strength Test Apparatus

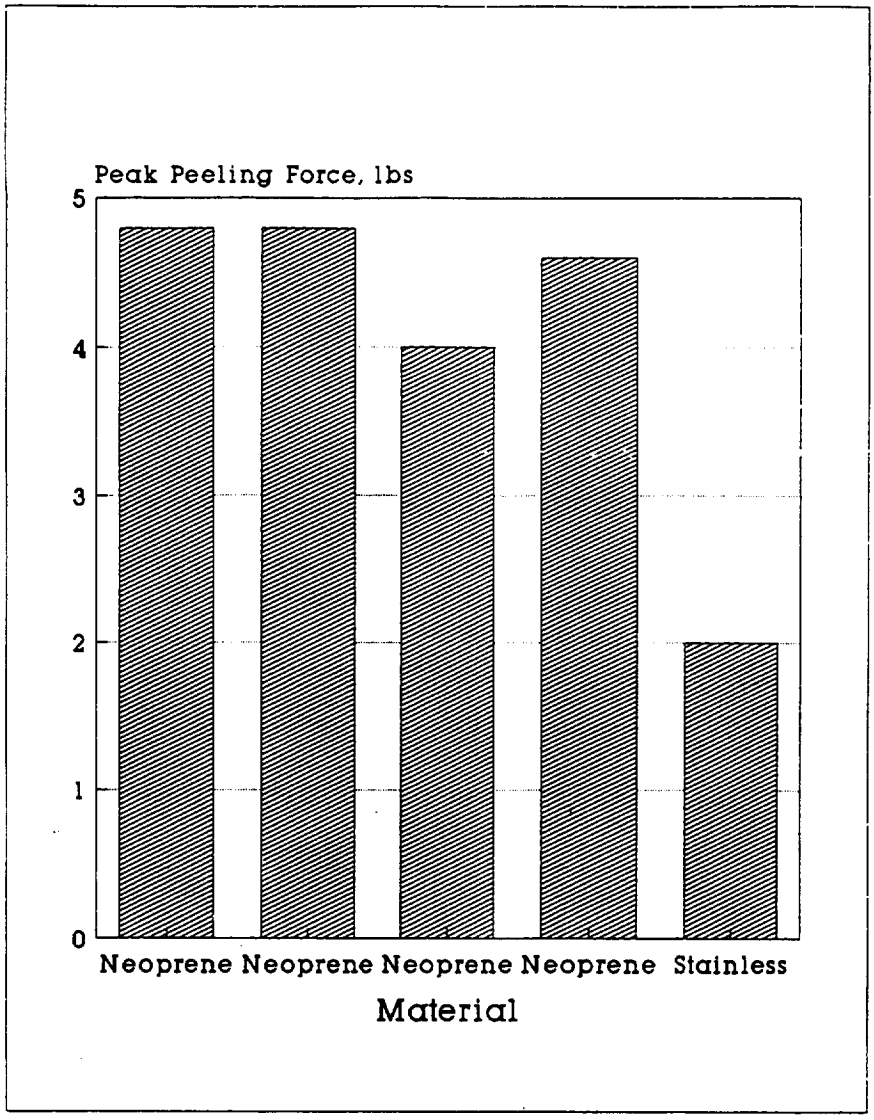


Figure 6 IRT Peel Strength Measurements

and electromagnetic blankets deicers operate with less than 2 degree peel angle. However, some laboratory data on natural ice with low peel angles were obtained.

In the laboratory tests of peeling, a small fixture was designed and built (Figure 7) for use in an environmental chamber in a 2,200 lb Instron tensile test machine. Most testing was conducted at 20° C. Peeling measurements from three specimens were made: neoprene, 0.003" stainless steel shim stock and .068" stainless steel shim stock. Results are plotted on Figure 8. For a 0° pull (direct shear) the shear stress on the thicker steel specimens approached the shear stress values measured with the NASA shear test apparatus. As the angle of pull increases, the peel force decreases. Since neoprene is less stiff than the stainless steel specimens, the decrease in peel load with the angle of pull is almost linear. Thus axial strains at the ice specimen interface affect failure as well as

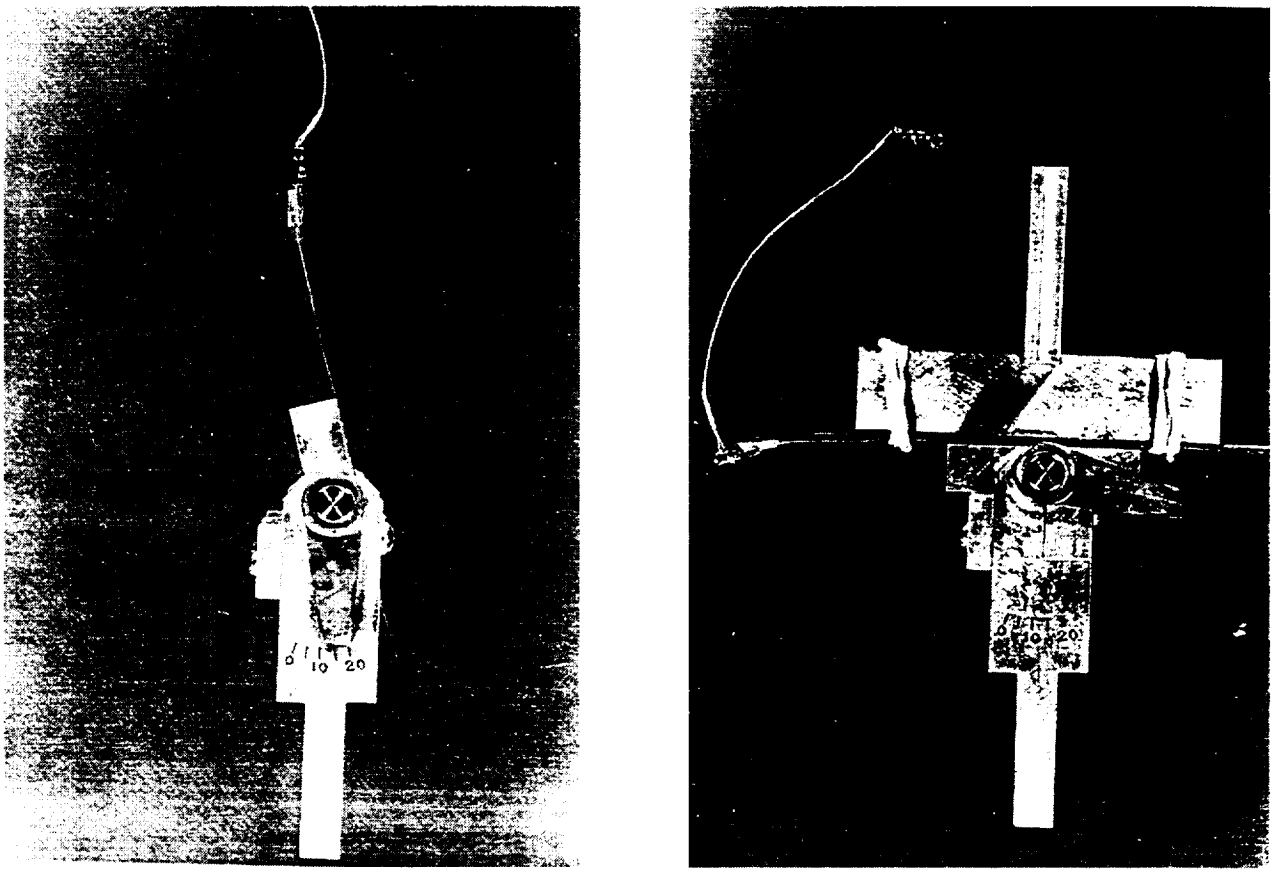

Figure 7 Natural Ice Peel Test Fixture

the angle of pull.

## 2.3 Bend Tests

Tension failures in the de-icing process are caused by the bending of impact ice. Therefore, tensile bending stress failures must be taken into account in the mathematical modeling of the de-icing systems. Preliminary tests were conducted on refrigerator ice coated metal substrates to determine the tensile cracking characteristics. Specimens were cracked using a STRESSCOAT strain indicator while food dye was used for a visual record of the cracked ice. Ice was built up on the specimen by freezing the aluminum substrate and then spraying water on it until the thickness was approximately 0.16 cm (1/16"). Specimens were then cracked at three different temperatures: -9° C, -18° C and -29° C (15° F, 0° F, -20° F). The first few tests showed that tensile failure was occurring in the area of high strains followed by shear failure at the metal-ice interface.

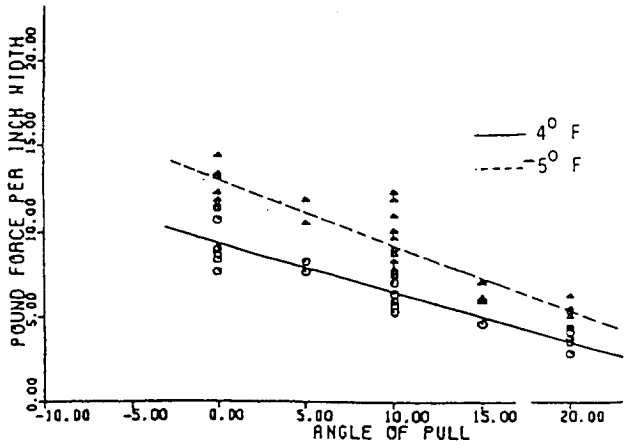


Neoprene Specimens

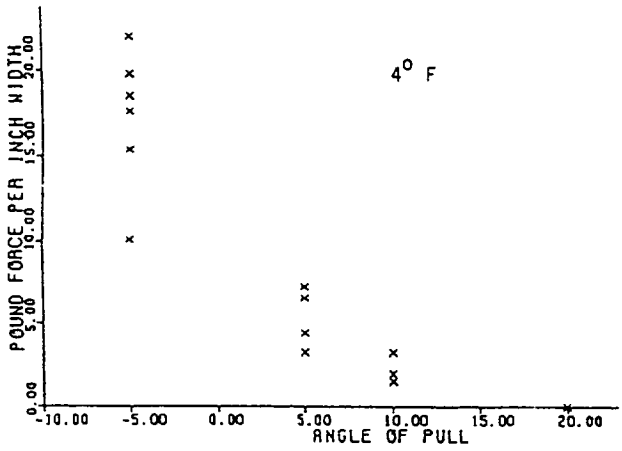


0.003" Stainless Shim Stock

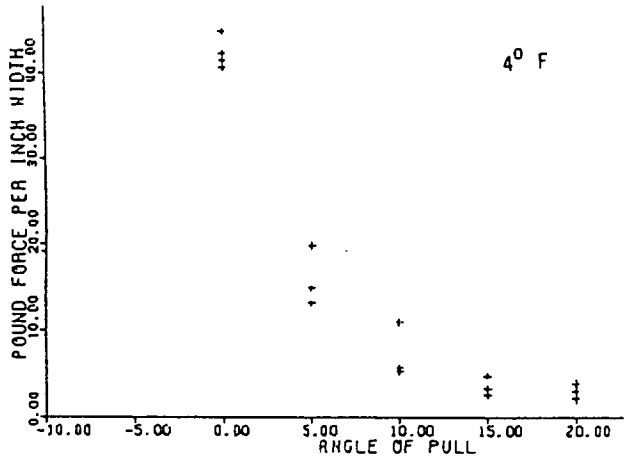


0.068" Stainless Shim Stock

Figure 8 Natural Ice Peel Strength Measurements

To prevent shear failure, the aluminum substrate specimens were sandblasted to roughen the surface and to increase the shear strength at the interface. This process reduced, but did not eliminate, shear failure at the interface. A typical specimen which failed in tension is shown in Figure 9.

## 2.4 Tensile tests

Tests on fresh water polycrystalline ice have been conducted by many researchers. Jellinek, in 1958, [23] froze fresh water between two metal cylinders to measure tensile properties. Hawkes and Mellor [22] in 1972 used dumbbell shaped molded ice specimens. Impact ice specimens developed by accreting ice on inch diameter split aluminum cylinders where used by Chu, Scavuzzo et al.[7,17,18] as well as by Druez et al. [24-26]. The split divided the cylinder into two halves so that the impact ice carried the applied tensile load. There was a

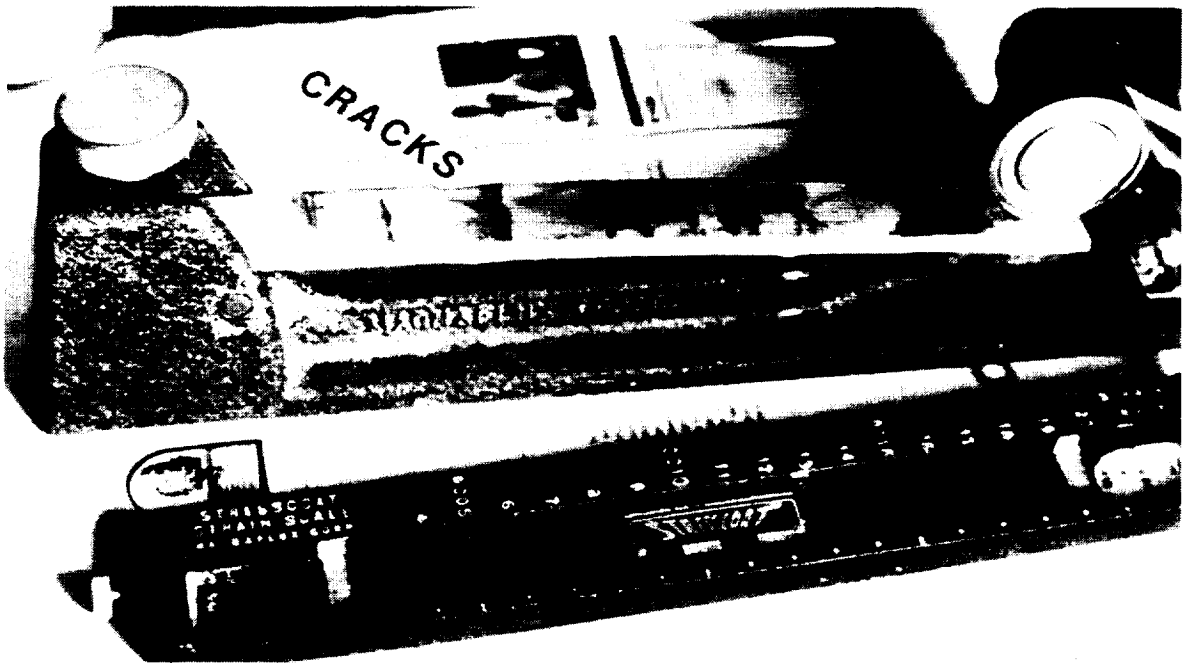


***STRESS COAT STRAIN INDICATOR***

ICE THICKNESS = 0.1"

DEFLECTION =0.625"

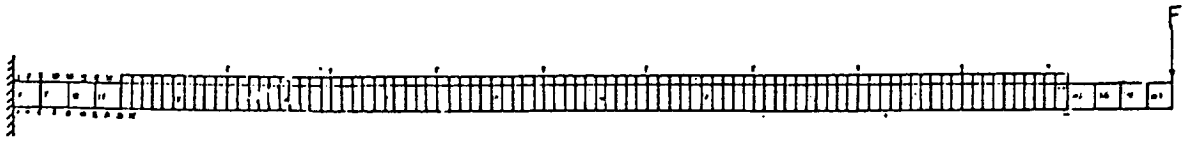

FINITE ELEMENT MODEL OF ICE COATED CANTILEVER BEAM

Figure 9 Bend Test Ice Tensile Failure

slight difference between the two cylinders; the surface of the Druez fixture was rough at the top and bottom and smooth over the center region around the split. The surface of the Chu-Scavuzzo cylinder was rough over its entire length. Thus, stress concentration effects were much higher in the Chu-Scavuzzo fixture and lower tensile strengths can be expected because of stress concentration effects.

Reich [20,27,28] used bend test specimens with and without a backing foil to determine both the tensile strength and elastic modulus. Data presented in the 1992 paper were conducted on pure impact ice beams. In order to obtain a uniform thickness, impact ice was first accreted onto a one inch wide foil, then cut to a uniform thickness and the foil removed. Then specimens were tested in three point bending to determine force-deflection curves to fracture. The flexural strength and elastic modulus were calculated from these data.

Hawkes and Mellor [22] measured a tensile strength of fresh water polycrystalline ice and established a value of 300 psi (2.1 MPa), a compressive strength of up to 750 psi (5.2 MPa), a tensile elastic modulus of $0.8 \times 10^{+6}$ psi (5.5 GPa) and a compressive modulus of $1.3 \times 10^{+6}$ psi (8.3 GPa) at -7° C. Results of this extensive test program show that the compressive strength is very strain rate sensitive. Furthermore, the compressive failure strength increases by a factor of four as the strain rate increases from $10^{-6}$ to $10^{-2}$ but the failure strain decreases by over an order of magnitude. These trends indicate that ice creep under compression is significant.

The mechanical properties of glaze ice are expected to approach those of fresh water ice. Rime ice, because of its lower density should be weaker and be more flexible (lower modulus).

The tensile strength from three point bend tests of an ice beam (without foil backing) varies with temperature. As the temperature decreases from -10° C to - 26° C the strength decreases approximately linearly from 1,000 psi to 250 psi [20]. The change from glaze to rime occurs about -18° C for a LWC of 0.5 gm/cm$^3$, MVD of 16 microns and an air velocity of 135 mph. The density of the impact ice also decreases below -18° C. The elastic modulus also follows the trend of the density. Creep is evident during the deflection of the ice beam. Thus, by using the elastic beam deflection formula,

$$\delta = PL^3/48EI$$

where

- $\delta$ - Beam center deflection (variable)
- P - Load (variable)
- L - Beam Length (6")
- t - Ice thickness (≈0.2")
- E - Elastic Modulus
- b - Beam width (1")

an effective elastic modulus that varies with displacement is calculated. Initially, for small displacements, the modulus of glaze ice should approach values obtained by Hawkes and Mellor. A value of $1x10^{+6}$ psi (6.90 GPa) was obtained from the beam tests which is about the mean of the tensile and compressive values measured on fresh water ice. The modulus of impact ice decreases to about $0.2x10^{+6}$ psi (1.4 GPa) for the least dense rime ice.

The flexural strength almost reaches 1,000 psi (6.89 MPa) for the glaze ice and decreases to 250 psi (1.72 MPa) for the coldest rime ice. These values exceed the tensile strength of fresh water ice published by Hawkes and Mellor[2] which is to be expected because of stress gradient and compressive effects.

Because of the differences in the tensile and compressive behavior of ice, bend testing leads to weighted values of the mechanical properties. Direct tensile and compressive testing lead to more direct measurements of strength and moduli.

Druez et al. [24-26] established a tensile strength of 360 psi (2.5 MPa) for what is believed to be glaze ice. The temperature was -14° C, with a LWC of 0.8 $gm/cm^3$, a MVD of 40 $\mu$ and a wind velocity of 10-16 m/s. The tensile strength decreased to approximately 60 psi (0.4 MPa) as the wind velocity increased, the strain rate increased and as the temperature decreased. Thus, as the ice tends to become rime its tensile strength decreases. Using the same technique, the compressive strength of impact ice was measured. Values varied from 1,200 to 1,450 psi (8-10 MPa) for a slow deformation rate of 0.45 mm/min but decreased to 450 psi (3 MPa) at a deformation rate of 26 mm/min. Druez et al. did not report measurements of either tensile or compressive moduli.

As indicated from the survey above there is a need for more tensile/compressive measurements of impact ice. There are many variables to consider such as strain rate, tension versus compression, temperature, rime or glaze ice or a mixture, wind velocity, droplet size etc. Based on the survey conducted during the winter of 1993 [20], recommended values are listed in Table 1.

**Table 1**
Mechanical Strength of Impact Ice

| ICE | TS MPa | CS MPa | $E_t$ GPa | $E_c$ GPa | Bending MPa |
|---|---|---|---|---|---|
| Glaze | 1-2 | 1-6* | 5-7 | 9 | 6.2 |
| Rime | 0.5-1 | 0.5-3* | 1.4-5 | 1.8-6* | 1.7 |

* An educated guess since there is no data.

where

TS - Tensile strength
CS - Compressive Strength
$E_t$ - Tensile Modulus
$E_c$ - Compressive Modulus Bending - Flexural Strength

## 3.0 ANALYTICAL STUDIES

### 3.1 Analysis of Rotating Airfoils

The basic objective of this analytical effort was to understand the tensile and shear stress distribution of impact ice adhered to a rotating airfoil. Itagaki [29] published one of the few analytical studies of this problem. In this work, it was assumed that normal tensile stresses and interface shear stresses exist simultaneously in the impact ice. Equations to predict ice fracture were determined by minimization of the equilibrium equations assuming that ice sheds when the centrifugal force equals the supporting forces developed by a combination of the shear and tensile stresses.

Finite element results led to a distribution of stresses very different from that assumed by Itagaki. For a uniform ice layer adhered to a rigid spinning airfoil, there are no normal stresses in the ice layer. The only stresses present are shear stress which reach a maximum value at the interface between the impact ice and rigid substrate and increase linearly from the center of rotation outward. Actually, no airfoil is rigid. However, the stiffness of an airfoil is usually much greater than that of the ice and, thus, to a first approximation the airfoil can be considered rigid.

The analytical finite element predictions in this work were made using the COSMOS/M software package. The basic assumption in these finite element analyses is that the axial strains in the rotating airfoil are developed before ice formation begins. Therefore, it is assumed that the airfoil is rotating and then impact ice is then accreted. The modeling technique used to simulate this condition was to assume that the airfoil structure has zero mass density. Due to this

assumption, axial strains in the airfoil structure are caused only by the added ice mass. Axial strains in the ice and airfoil must be equal; stresses are not equal because of the difference in elastic modulus of the ice and substrate. If the airfoil is assumed to be aluminum, axial stresses in the ice caused by this added mass are a factor of ten lower than the airfoil stresses. As long as this added accreted ice mass is a small percentage of the rotating airfoil mass, the axial stresses in a uniform ice layer are not significant.

A solid eight nodded element was used in the modeling of both the ice and the structure. A number of models were developed and analyzed: the button model; the uniform ice layer; the shear crack in a continuous ice layer; approximate rime and glaze ice on OH-58 rotor; and, an actual ice profile on OH-58 tail rotor. Details of the results of these models are presented in References [10,11,21].

Composite elements were considered and discarded because of limitations with the method of mass distribution in the element for dynamic problems. In a composite element both the ice layer and substrate can be modeled. For static loads, stresses in each layer and overall deflections of the composite can be easily determined. However, for dynamic problems, the inertia of all layers of the composite element is lumped onto a reference plane. Thus, differences in stresses between the ice and substrate caused by rotational accelerations can not be calculated. As a result, eight noded solid elements were used to model both the ice and substrate as shown on Figure 10.

The most significant results of this study are listed below:

(1) If the rotating airfoil is rigid compared to a uniform impact ice layer, the shear stress at the interface of the ice and substrate can be approximated by the "button" equation

$$\tau = \rho\omega^2 Rh$$

Thus, the shear stress increases linearly with the radial position on the airfoil R and with the ice thickness, h. There are no axial stresses in the ice. Finite element results are shown on Figure 11.

(2) Since the maximum shear stress occurs at the outer tip of the airfoil, it is assumed that failure will be initiated as a shear crack at the ice/substrate interface and propagate inward. This condition was modeled with finite elements using the model also shown on Figure 10. Cracks were modeled at the airfoil-ice interface at the tip by using coincident nodes on these elements and modeling a crack. Calculations indicate that very high shear and tensile stresses are developed at the crack tip that will lead to tensile fracture of

the impact ice. These tensile stresses increase very rapidly with the length of the shear crack (Figures 12,13). As a result, it is predicted that small ice chunks will shed from the airfoil when the critical shear stress is reached. This type of fracture has been observed experimentally. However, additional work is needed on the modeling of experimental ice shapes before more definite conclusions can be made.

In summary, the analysis begins with a simple button model that seemed to approximate the expected average shear stresses. Next, the model was complicated by adding a continuous layer of ice. As the model was idealized, the shear stresses approached the theoretical values expected. However, this report shows that the tensile stress approaches zero in the ice when it is continuously bonded to the blade. When a shear stress crack is introduced into the continuous ice layer model, it became evident that tensile stresses are the mechanism of failure after shear cracks propagate to approximately one inch in length.

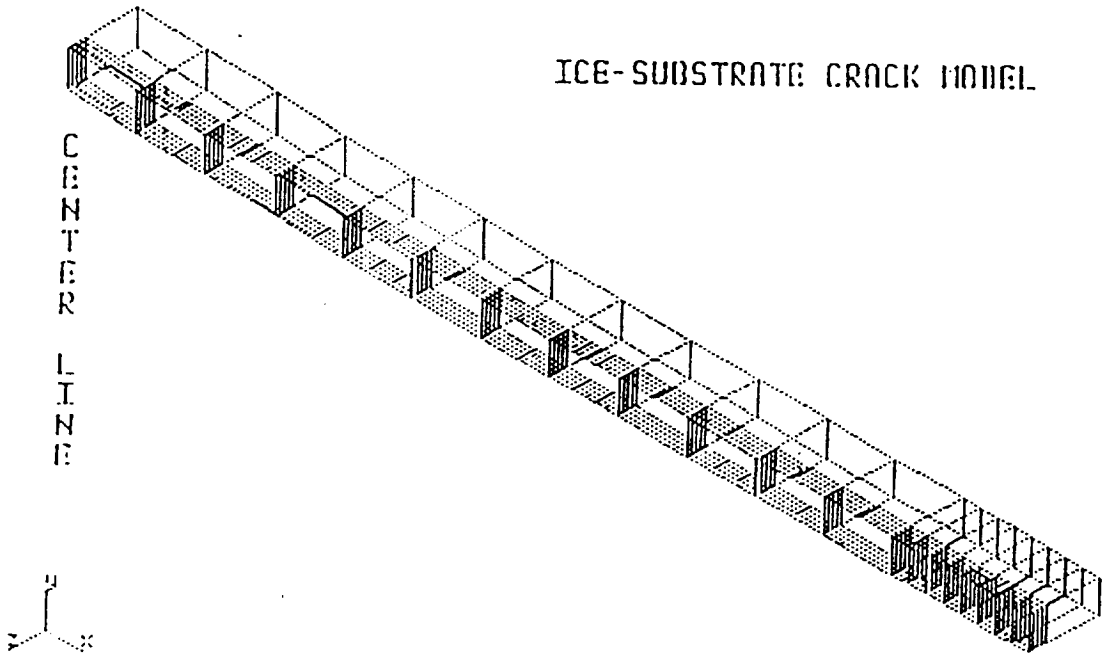


Figure 10 Finite Element Model of an Idealized Rotating Airfoil

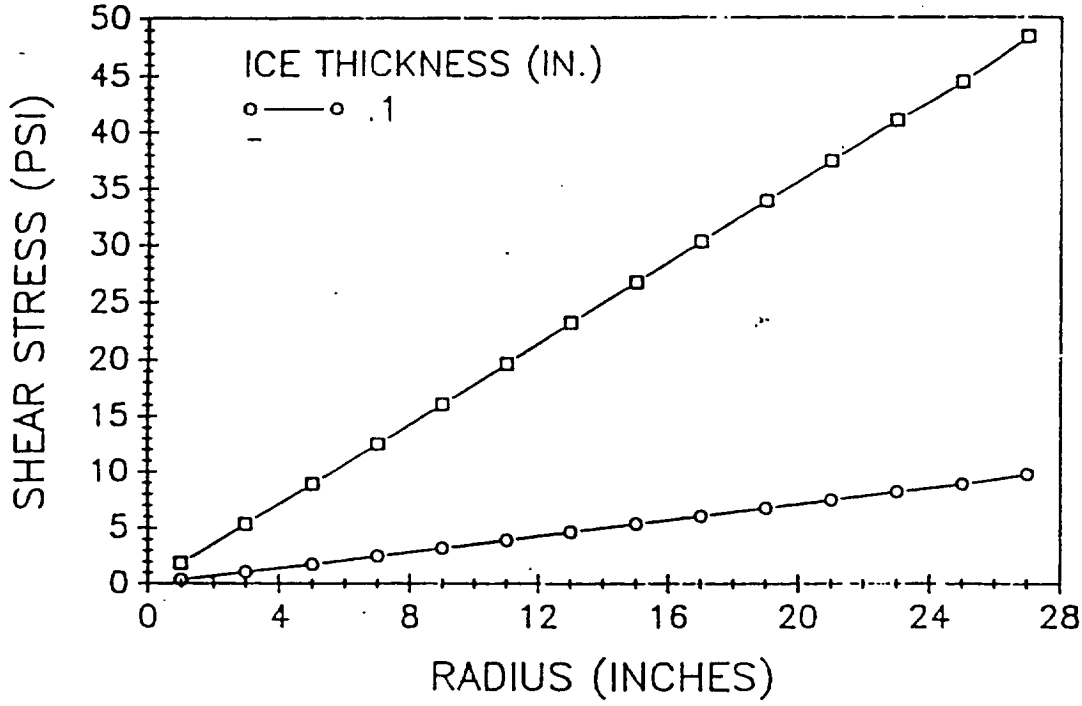


Figure 11 Linear Interface Shear Stress in a Rotating Airfoil with a Uniform Ice Layer

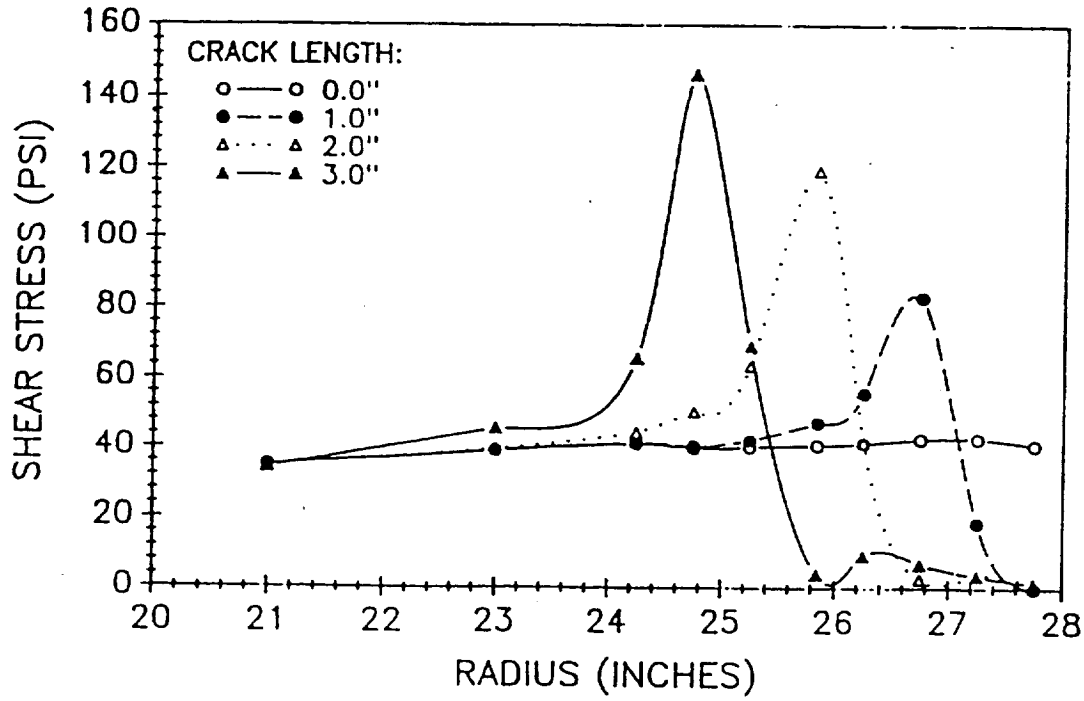


Figure 12 Shear Stress Concentration Effects at Crack Tip

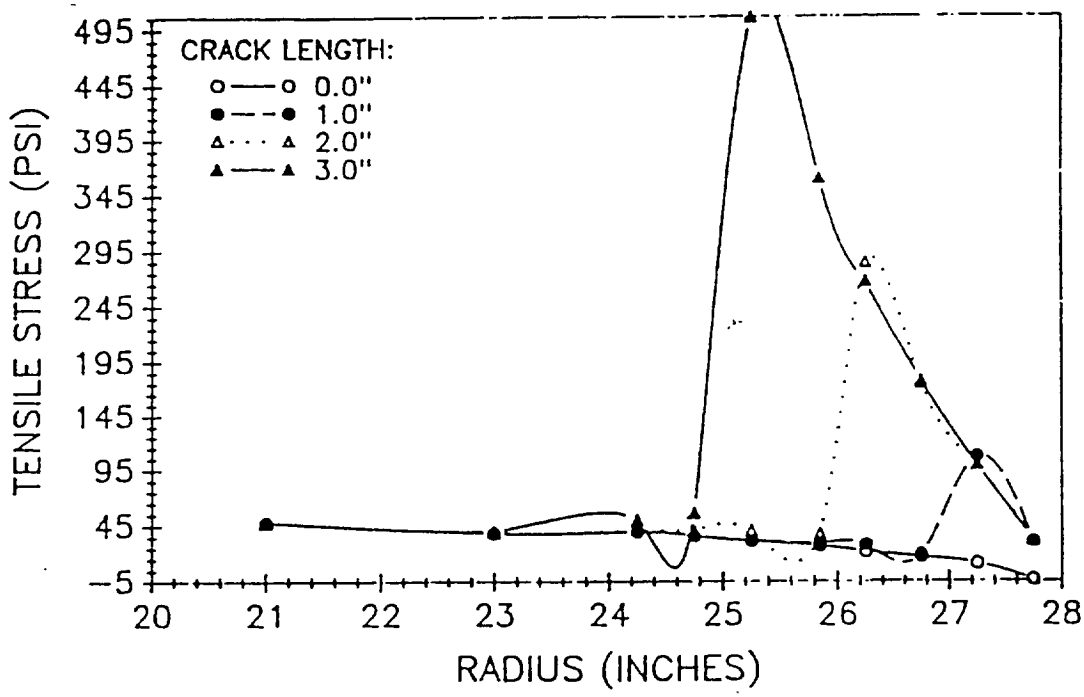


Figure 13 Normal Stress Concentration Effects at Crack Tip

Approximate glaze and rime ice formations added to an OH-58 rotor profile yielded stress distributions that were similar although the magnitude of the glaze ice stresses were higher. When the actual ice formation was analyzed, the stresses calculated approached those expected for a glaze ice formation. Adding lift forces to the airfoil caused bending of the blade that increased the magnitude of shear stress indicating that these loads must be included in the deicing analyses of helicopter blades.

## 3.2 Statistical Structural Analysis

In order to perform a statistical structural analysis, the best fit statistical distribution for the shear strength data was used in combination with a shear stress distribution calculated by the finite element analysis for the actual ice profile. By assuming a statistical distribution for the calculated shear stress values, a probabilistic combination of the two independent distributions can be utilized to calculate the probability of ice shedding. The OH-58 data collected included ice tracings that were used in the forgoing analysis. An ice tracing that was taken after a run that involved shedding that was approximated by COSMOS/M finite element program, and a stress analysis was completed. This particular ice shape was taken from a run in which the wind velocity was recorded as 70 mph and droplet size was determined to be fifteen microns. At

this point, it was assumed that the calculated shear stress of ice had a normal distribution. To find the parameters for this distribution, the shear stress values generated by the finite element analysis for the inside elements at the leading edge were averaged together, and the mean and standard deviation were found to be:

$$s = 26.4 \text{ psi}$$
$$\sigma = 0.873 \text{ psi}$$

As the affect of lift was added to the model by including a pressure load, the mean, s, and standard deviation, $\sigma$, of the inside elements at the leading edge were calculated as:

$$s = 42.9 \text{ psi}$$
$$\sigma = 5.85 \text{ psi}$$

It was determined earlier that the best fit statistical distribution for the experimental shear strength of ice was the Weibull distribution. From the data collected, the case in which the wind speed was 50 mph and the droplet size was 15 microns best duplicated the conditions of the OH-58 run. There is no definable trend for the shear stress as a function of wind speed, so no adjustment was made for this difference. Therefore, the parameters for the shear strength data distribution are:

$$S = 48.0 \text{ psi}$$
$$\sigma = 10.1 \text{ psi}$$
$$x_0 = 35 \text{ psi}$$
$$b = 1.3027 \text{ psi}$$
$$\theta = 49.1 \text{ psi}$$

The probability of shedding is based on two independent quantities; the shear strength of the ice and the shear stress in the ice. If S denotes the adhesive shear strength of ice and s represents the shear stress in the ice induced by centrifugal force of rotation and lift at the tip of the rotor, then the random variable y is related to the probability that the ice will not shed by:

$$\begin{aligned} P &= P(S > s) \\ &= P\{(S-s > 0\} \\ &= P(y > 0) \end{aligned}$$

where: $y=S-s$ = stress difference random variable

Figure 14 illustrates the concept of interference for the two independent random variables for the cases in which there is no lift and then with lift taken into account, respectively. The interference area indicates graphically the probability of failure. To determine this probability of failure, the concept must be developed analytically. The non-shedding reliability is the probability that the shear strength is greater than the stress for the possible range of the stress values. This is expressed as:

$$R = \int_{-\infty}^{\infty} f_s(s)\left[\int_{s}^{\infty} f_S(S)dS\right]ds$$

The unreliability is the probability of failure, or in this case, the probability that the ice will shed. The probability of failure is computed by:

$$R = 1 - \int_{-\infty}^{\infty} f(s)[1 - F_S(s)]ds \quad = 1 - R = P(S \leq s)$$

$$= \int_{-\infty}^{\infty} F_S(s) f_s(s)ds$$

where: $F_s(S)$ = cumulative density function for shear strength

$f_s(s)$ = probabilistic density function for shear stresses

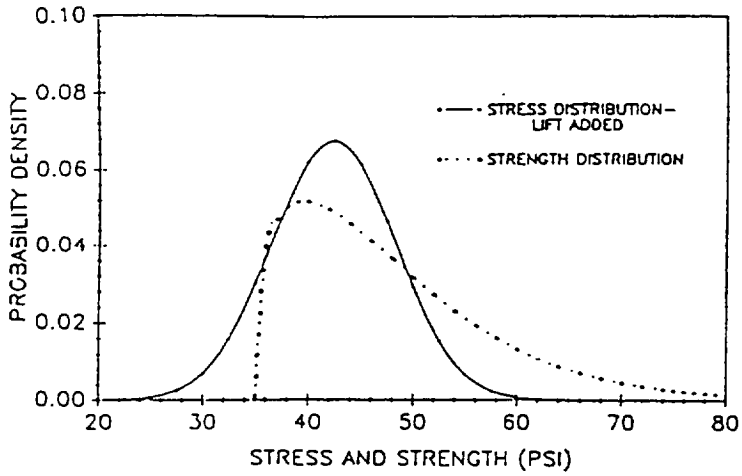


Figure 14 Stress-Strength Statistical Structural Interaction

In this case, the shear strength (S) of the ice follows a Weibull distribution. It was assumed that the shear stress followed a normal distribution. Substituting in the Weibull cumulative density function and the normal probabilistic density function, the probability of failure becomes:

$$P(S<s) = \int_{S_0}^{\infty} \frac{1}{\sigma_s\sqrt{2\pi}} exp[-\frac{s-\mu_s}{2\sigma s^2}\, ds -$$

$$\frac{1}{\sigma_s\sqrt{2\pi}} \int_{\delta_0}^{\infty} exp\{-[\frac{s-\mu_s}{2\sigma s^2} - (\frac{s-s_0}{\theta - S_0})^b]\}\, ds$$

Substituting the appropriate transformation, the first integral represents the area under the standard normal density curve from

$$z=(s-\mu_s)/(2\sigma^2)$$

to positive infinity. This area is denoted by:

$$1-\Phi\left(\frac{S_0'-\mu_s}{\sigma_s}\right)$$

and can be found using a standard table in any statistical handbook. Introducing further transformations and substituting, the probability of failure is expressed by:

$$P(S<s)=1-\left(\left(\frac{S_0-\mu_s}{\sigma_s}\right)-\frac{1}{\sqrt{2\pi}}\left(\frac{\theta-S_0'}{\sigma_s}\right)\right.$$

$$\int_0^{\infty} exp\left[-y^b-\frac{1}{2}\left\{\left(\frac{\theta-S_0'}{\sigma_s}\right)y+\left(\frac{S_0-\mu_s}{\sigma_s}\right)\right\}^2\right]dy$$

Numerically integrating this expression when the mean and standard deviation are 24.4 psi and 0.873 psi, respectively, by Simpson's rule with end correction, the probability that the ice will shed was found to be very close to zero. Next, the case in which lift was taken into account was evaluated on the basis of interference. The probability of shedding using the appropriate mean and standard deviation lead to a value of 36.6 percent. Table 2 shows the relationship between increasing mean and standard deviation to the probability of ice shed. Given the small sample sizes and estimated stress distributions, a ten percent variation in the calculations is possible. After examining the OH-58 test data, it was found that two out of eleven cases shed for test runs in which the ice formation had the approximate thickness of the ice formation modeled by COSMOS/M. However, the two cases that did shed had angles of attack of four and eight degrees. Therefore, the experimental probability of ice shed was found to be zero when the angle of attack was zero but was calculated as 18.2 percent when the angle of attack was between four and eight degrees. If the calculated stresses are reduced from 42.9 psi to 40 psi, the probability of failure is reduced from 37 percent to 24 percent, which is close to the value determined from the OH-58 experimental data of 18.2 percent.

It can be concluded that the shear strength data is best represented by a Weibull distribution. The concept of interference was applied to two random variables of shear load stress and shear strength of accreted ice to find the

probability of shedding. This method seems to yield somewhat dependable results when compared to the OH-58 experimental results. When the angle of attack is zero, and hence, no lift present, the probability of ice shed is computed a zero both theoretically and experimentally. When the effects of lift were added to the theoretical model and the interference is calculated with a new mean and standard deviation, the probability of ice shed is calculated as 36.64 percent. This value is significantly larger than the OH-58 experimental results, although if ten percent uncertainty of the finite element generated stresses is taken into account, the calculated probability of failure is approximately equal to the experimental value (18.2%). It should be mentioned that the aerodynamic forces and the unsymmetrical ice loading which constitutes aerodynamic forces imposed on the rotor are not considered. Taking these forces into account would have increased the mean shear stress acting on the ice and hence, increased the probability of shed slightly. However, the discrepancy between theory and experiment could be largely attributed to an inadequate number or experimental data points for statistical analysis.

## 3.3 Analysis of EIDI Systems

An approximate finite element model of an airfoil section fitted with an EIDI system was developed to compare measured deflections with calculated values and to predict the ice shedding area. The airfoil surface and ice was modeled as two layers of plate elements which represent the aluminum skin and the impact ice layer, respectively. Weightless, stiff beam elements were used to connect the two layers of plate elements and to obtain the shear stresses at the aluminum-ice interface. Both the plate elements and the beam elements were assumed to have materials with linear, temperature independent isotropic properties. The node points at the edges of the airfoil were constrained in all six directions. All other node points were constrained in all rotational directions. Without this constraint, convergence could not have been obtained. Shear between the two plates was carried by the beam elements.

The structural model was excited by an analytically determined force-time history input. To determine the force-time history, the skin of the airfoil was assumed to be a flat circular plate. The plate was assumed to be a current-carrying conductor loop, and the aluminum skin was subdivided into thirty-six circular loops. Each current-carrying loop produced magnetic flux that linked all the other loops. At each step of the solution, the differential equations of all the current loops were solved simultaneously. From the value of the flux density and loop currents, the forces on any loop could be calculated. In particular, the forces on current skin loops could be obtained and divided by loop area to give the values of pressure. If the total force on the aluminum skin was multiplied by the time increment and summed for the total time period of interest, then the impulse was obtained. The

calculated final value of the impulse compared very well (less than 5 percent error) with Boeing laboratory data using an EIDI coil on a ballistic pendulum. The calculated values of impulse also agreed well for other materials, such as titanium and stainless steel, which were tested during this project.

Displacement-time histories of the bending waves developed by the EIDI coil were measured along both the transverse and lateral directions. The calculated displacement-time histories were compared with the desired displacement-time motion. Various values of viscous damping were introduced into the program inputs to account for energy dissipation associated with ice shedding. Damping values of 0, 5, and 10 percent were examined. The best correlation between the desired displacement-time history and the calculated displacement-time history and stress response was obtained with 5 percent damping.

Shear stresses in the beam elements were studied and were used to calculate the shear forces at the interface. One quarter of the area of all the four elements was used to determine the interface shear stress from the beam shear force. Time history plots of shear stresses in the upper left quadrant of the airfoil along the cord and axial directions at specific grids were calculated. Failure was assumed to occur if this stress reached 50 psi. Peel deflections along the leading edge were compared to measured values [12]. Agreement is reasonable. Calculated defections along the chord direction decreased much more rapidly as the bending wave traveled around the leading edge. Furthermore, initial deflections at some points were in the negative (inward) direction of the airfoil. This trend was also observed in the measurements. After about one millisecond, deflections at some points began to increase in a divergent manner, which indicated numerical instability in the calculations. Because of the rapid loading, time steps of one microsecond were specified, which lead to significant instability after 2 ms.

Shear stress plots indicate that ice shedding is predicted along the six inch length parallel to the leading edge. Failure is not predicted at about four inches from the coil. This appears to agree with the measurement of the actual airfoil's region of ice shedding. However, at six inches from the coil, stress exceeded the critical value of 50 psi,which indicates ice shedding; this does not agree with measurements. However, there appears to be an instability in the analysis that makes this calculated result questionable.

## 3.4 Analysis of Shear Tests

A finite element study of the shear test specimens was conducted in order to access the magnitude of stress concentration effects on the two types of test specimens: the rectangular window and the square window. Intuitively, it was felt that stress concentration effects associated with the rectangular window specimen would be less than those of the square window specimen. As a result, finite element models were developed for each type of specimen for both a relative and

absolute evaluation of these stress concentrations.

Two sets of boundary conditions were specified for each specimen type. First, it was assumed that the ice was fixed to all edges of the window in the outer cylinder. In the second case, it was assumed that the ice accretion was fixed along the two sides of the rectangular windows and to the two sides and bottom of the square window. The second set of boundary conditions was believed to be more realistic and the results of these two analyses are present in Figures 15 through 18. For the square window, it is assumed that tensile failure will occur between the top and bottom flanges and outer cylinder. As a result, there is no support along either the top or bottom edge of the ice accretion on the rectangular window.

Figures 15 and 17 show the normal and shear stress distributions, respectively, for the square windows. As can be seen, there are significant shear stress concentrations at the boundary of the accreted impact ice and outer cylinder. The normal and shear stress distributions for the rectangular window are plotted on Figures 16 and 18, respectively. From these results, it can be seen that the stress concentration effects appear to be even larger than those for the square window. Thus, the modification did not lead to a more uniform shear stress between the inner cylinder and impact ice. Test results indicated that the average shear stress from the two types of specimens were not statistically different.

In conclusion, shear stress concentrations based on the average shear stress of 4.3 and 5.9 were determined from the finite element study. This effect probably reduced the measured average adhesive stress approximately by a factor of 2. Stress concentrations of this type will occur with any shear testing. De-icing systems, however, do take advantage of stress concentrations to effectively debond the ice.

## 3.5 Aerodynamic Forces

Impact ice formations on airfoils are subjected to various forces during normal aircraft operation. Stresses that develop at the accreted ice and metal substrate interface during normal operations are caused by the following sources:

(1) flexing of the aerodynamic surface caused from structural vibration and aerodynamic forces
(2) direct loading of aerodynamic pressure forces acting on the ice
(3) inertia forces in the case of rotating propellers of blades
(4) thermal stresses developed from phase changes and thermal gradients in the accreted ice

If stresses from these sources exceed a critical value, shedding results. Using finite element analysis, the stresses from these aerodynamic loads were evaluated and related to the fracture strength of impact ice. The ice geometry used in the finite

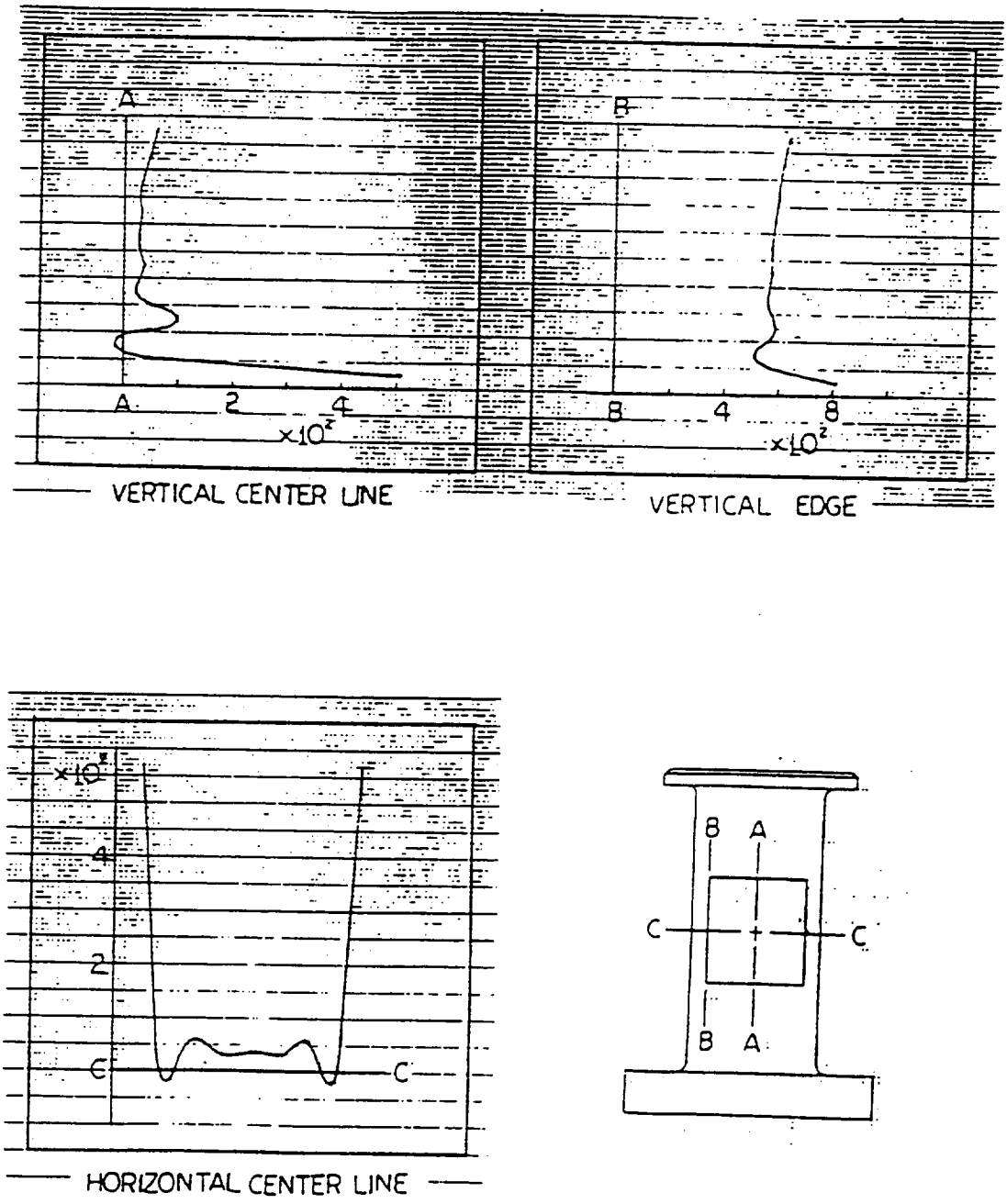


Figure 15 Shear Stresses in Specimen Square Windows

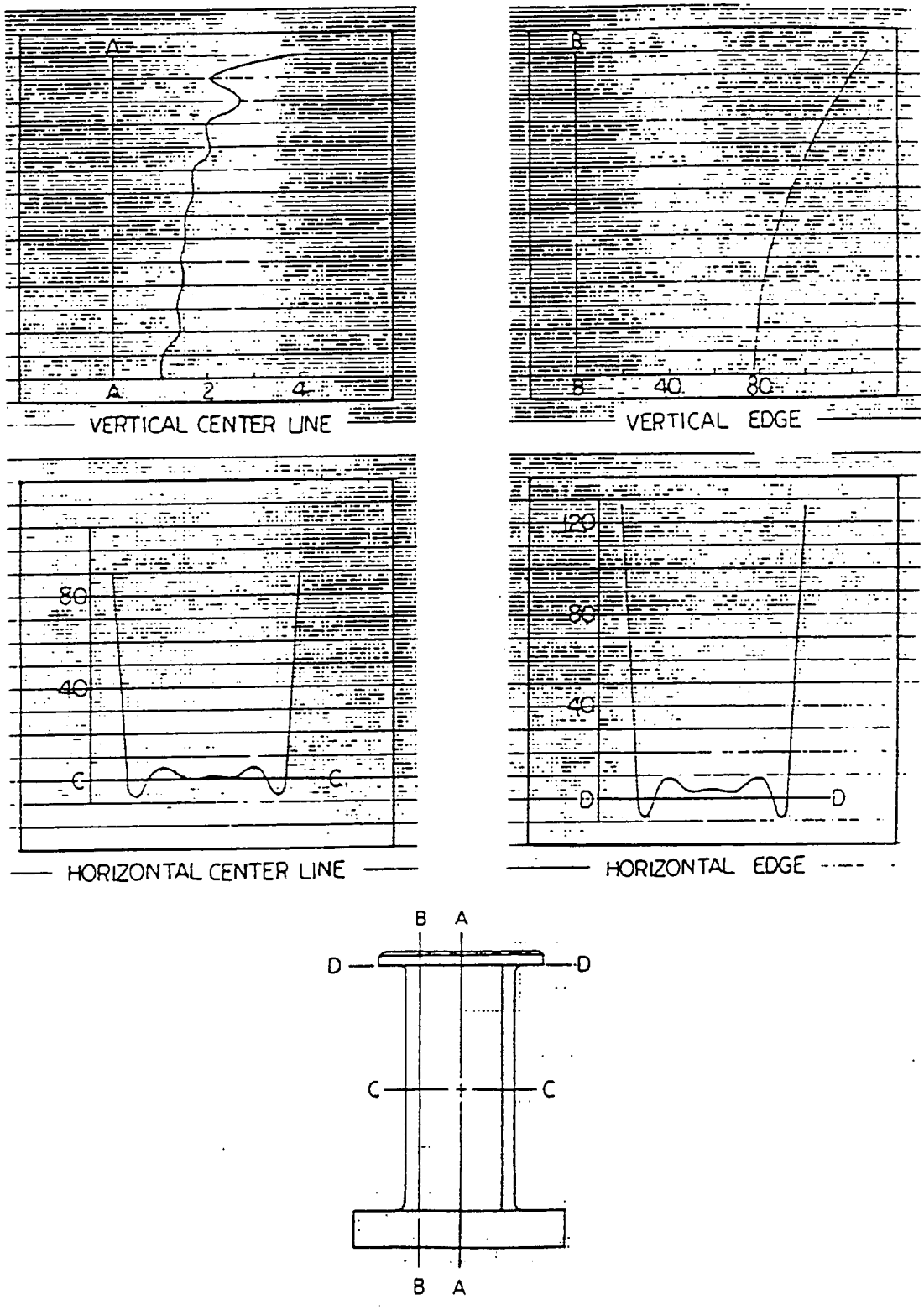


Figure 16 Shear Stresses in Specimen Rectangular Windows

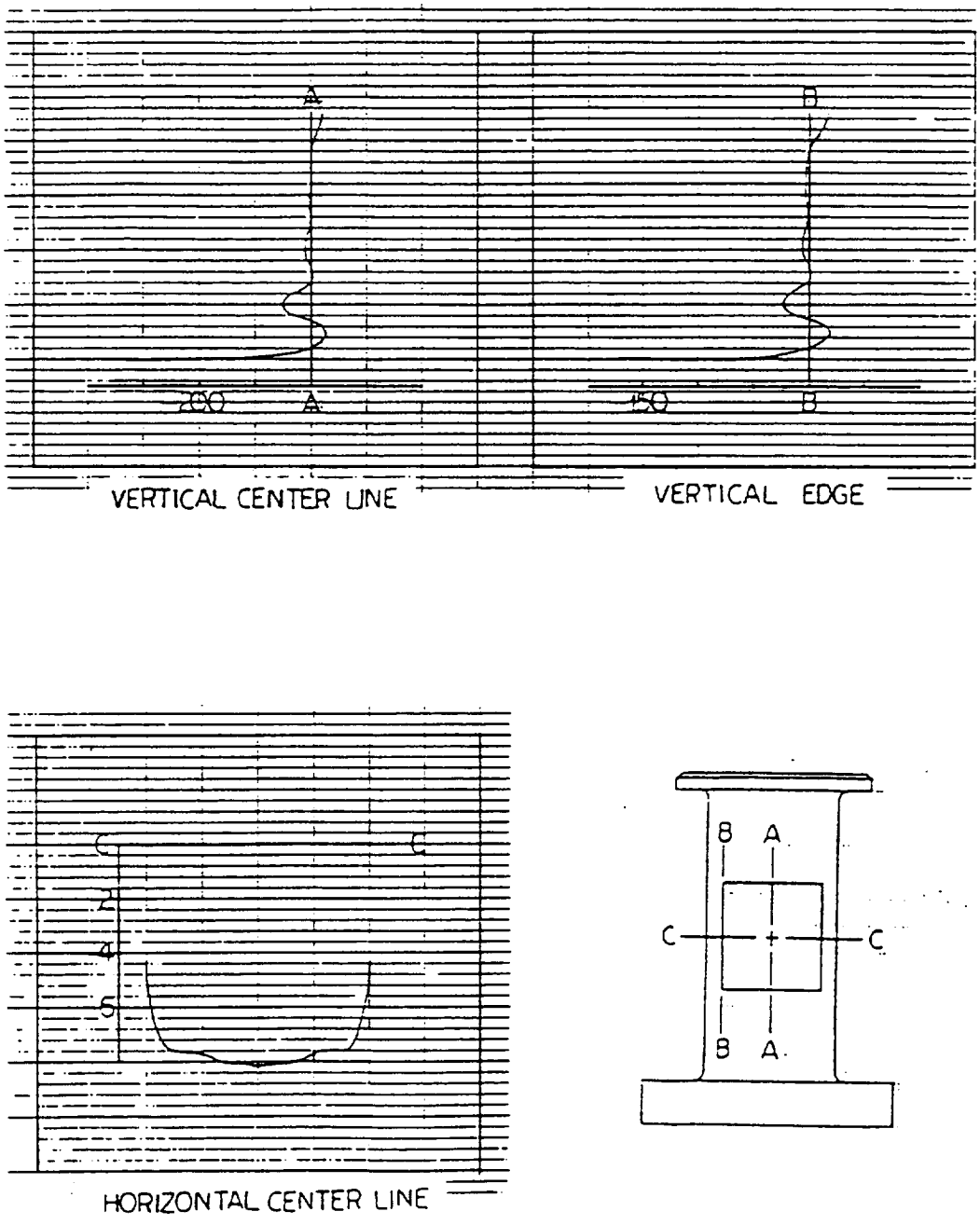


Figure 17 Normal Stresses in Specimen Square Windows

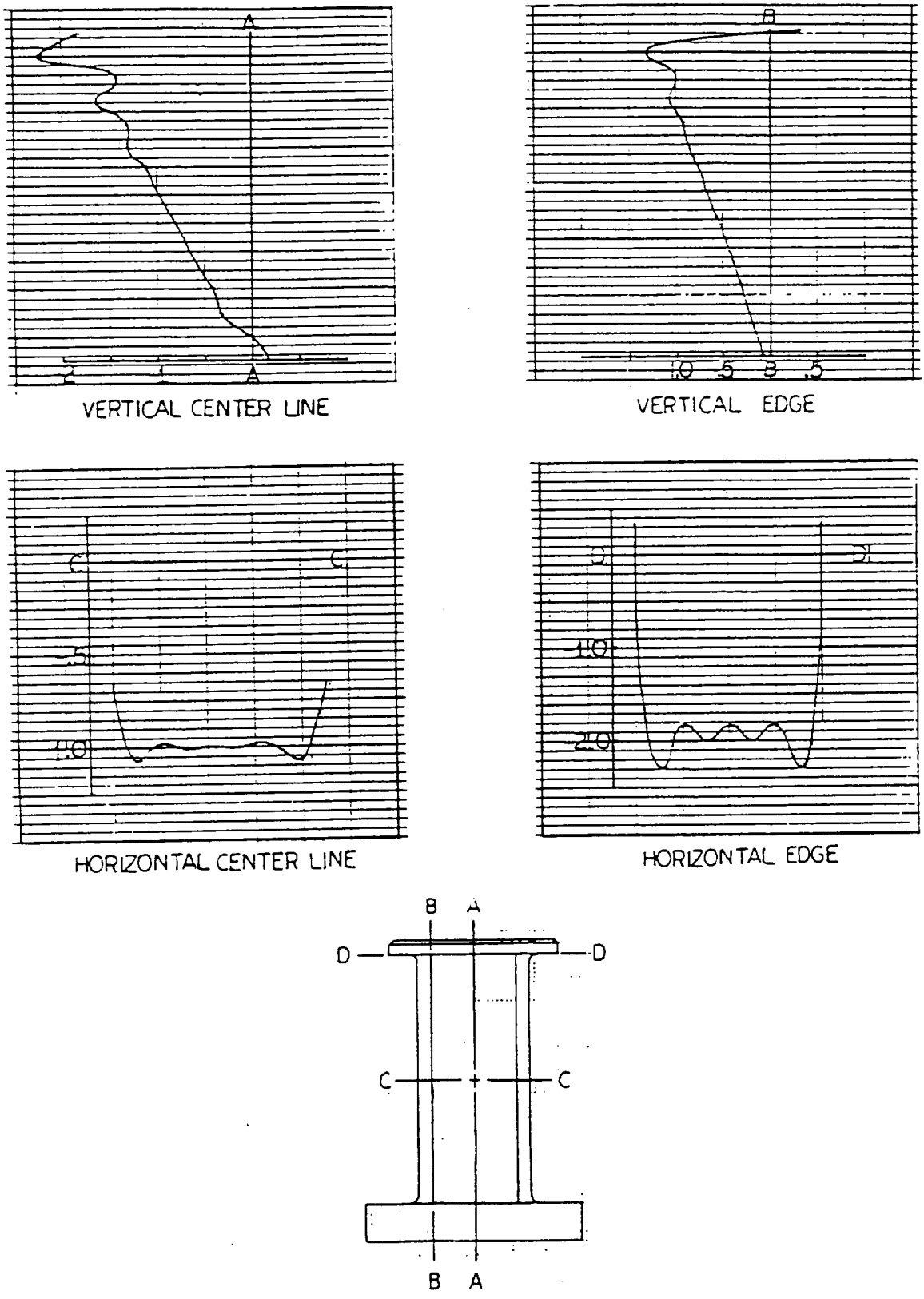


Figure 18 Normal Stresses in Specimen Rectangular Windows

element analysis was a glaze ice shape on a NACA 0012 airfoil. This well defined geometry consisted of circular arcs and line segments which facilitated easy mathematical modelling.

A plane two dimensional finite element model was developed for the analysis using the PC ANSYS finite element program. This code was chosen because it has excellent graphic capabilities, is interactive and is easy to use. Considering the curved shape of the ice and the airfoil, six noded higher order plane stress triangular elements were employed to generate the mesh through the automesh generation routine available with the ANSYS package. This element has a quadratic displacement behavior and is well suited to model irregular meshes. All the nodes at the interface between the ice and the airfoil were constrained for zero displacements and rotations. The airfoil was considered to be rigid. Thirty six elements were used to model the impact ice geometry, as seen in Figure 19. The pressure coefficients were calculated by a computer code which solves the Navier-Stokes equations in two dimensional for the flow field characteristics around the iced airfoil. These pressure coefficients have been correlated with experimental measurements and were found to be in good agreement. Pressures were applied normal to the element faces. Negative pressure (suction) acted normally inward to the ice. Positive pressure always existed at the stagnation point of the leading edge of the accreted ice shape. At an angle of attack of zero degrees, negative pressure existed above and below the ice shape. As the angle of attack increased, the pressure acting on the bottom edge of the ice became more positive because of the smoother flow of the air over the bottom edge. On the upper edge, the pressure became more negative as the angle of attack increased. It should be noted that the pressures increased approximately as the square of the velocity.

Pressure loadings on the accreted ice were calculated at Mach numbers of 0.12, 0.3, and 0.6. For a Mach number of 0.12, the angles of attack investigated were 0, 2, 4 and 6 degrees; whereas for a Mach number of 0.3 and 0.6, the analyses were run only for a 0 degree angle of attack.

Stresses varied significantly at the interface between the impact ice and airfoil surface (Figure 20). Peak shear stresses at the interface as a function of Mach number and angle of attack are plotted in Figure 21. The maximum stresses occurred at a Mach number of 0.6 and varied linearly as the square of the Mach number. The stresses at airfoil velocities below 0.3 are in the order of fractions of one psi and, therefore, are not significant. The shearing strength of ice has been determined to be typically between 40 psi and 60 psi. At a Mach number of 0.6, the maximum shear stress was found to be about 9 psi, which is about 20 percent of the shear bonding strength. The maximum normal tensile stress for the same case was also found to be about 9 psi and the maximum principal stress was found to be in the range of 8 to 10 psi. Stresses reached about 10 percent of the shear debonding strength at a Mach number of 0.45. Variation

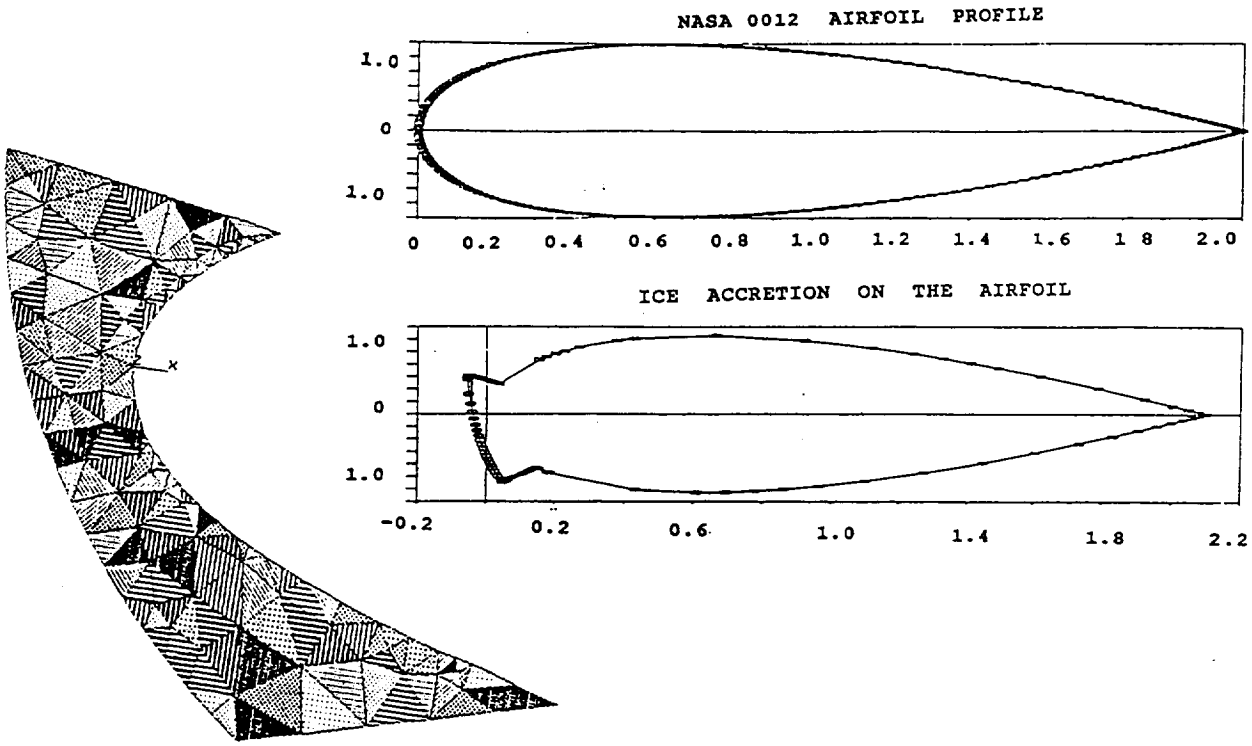


Figure 19 Airfoil Profile and Two-Dimensional Finite Element Model of Impact Ice Adhered to an Airfoil

of the interface shear stress with the angle of attack was about a factor of 2.5 at 0 degree angle of attack and a Mach number of 0.12. The maximum value occurred at an angle of attack of 4 degrees.

The stresses at air velocities of less than a Mach number of 0.45 were insignificant and were not expected to contribute to ice shedding. However, for a Mach number of 0.6, the maximum shear stress was about 20 percent of the ultimate shear debonding strength. Shear stresses at the impact ice airfoil interface varied about a factor of 2.5 as the angle of attack increased from 0 degrees to 4 degrees. Thus, at high speeds and at a high angle of attack, stresses from direct aerodynamic loading must be considered in the analysis of stresses of impact ice accreted on aerodynamic surfaces.

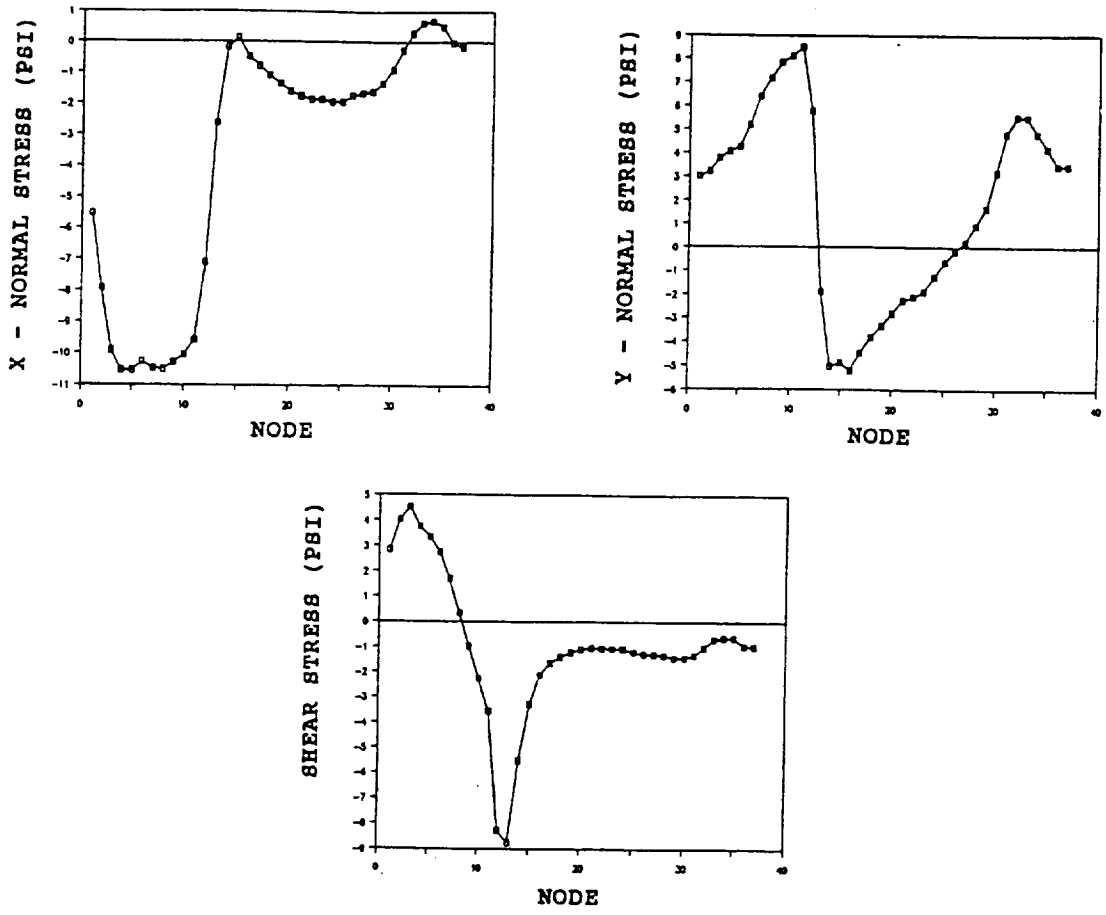


Figure 20 Typical Interface Stresses (Mach Number = 0.6 and 0° Angle of Attack)

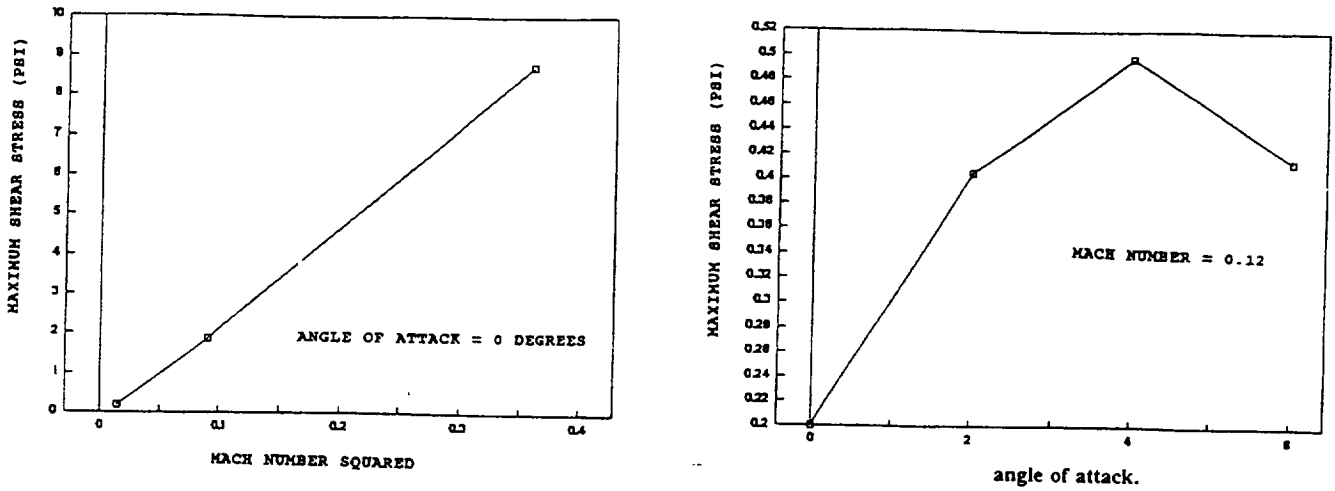


Figure 21 Peak Shear Stresses Versus Mach Number and Angle of Attack

## 3.6 Analysis of Bend Tests

To effectively model the bending fracture tests, the ADINA program was used since it has a concrete fracture model that can be used to model the fracture of brittle materials such as ice. In order to model the beam bend test specimen described in Section 1.3, the tension strength of ice had to be specified, and a value of 690 * $10^3$ $N/m^2$ (100 psi) was chosen. The finite element model of the aluminum beam-ice composite is shown in Figure 9. After reducing the load steps drastically because of convergence problems in the fracture model, the model predicted the interval of cracking approximately 1.3 cm (0.5") along the length of the beam, which agrees reasonably well with observed fracture.

At a later time in the grant, this finite element analysis was redone using one of the linear solution sets of COSMIC NASTRAN. In this work the same analytical model, shown in Figure 9, was used. However in this case, the model was run as a linear analysis and the highest bending stress in the ice identified. Then a crack through the ice thickness at this location was modeled by adding a coincident node point on the outer (top) edge of the model and redefining the adjacent elements. In this manner a crack was added to the grid. The problem was then rerun and the process repeated. The crack pattern obtained in this manner was identical to that developed with the nonlinear ADINA code. Of course in this case there were no convergence problems or long run times that experienced with ADINA. This quasi-linear analysis using NASTRAN ran quickly and compared well with the experimental data.

## 3.7 Approximate Formulas for Interface Shear Stresses

It was request that approximate formulas be developed to approximate the shear stresses in airfoils from the various load acting on the accreted ice. As shown in this work, forces acting on impact ice that develop stresses tensile and shear interface stresses include aerodynamic loads, centrifugal force on rotating airfoils, and stresses caused by the flexing and twisting od airfoils. In addition, residual stresses in the ice are developed during the accretion process. The super cooled droplets impact the ice surface and either flow and freeze for glaze ice of freeze on impact for rime ice. In either case, the change in density associated with freezing as well as the thermal gradients cause residual stresses to be developed in impact ice. Furthermore, ice creeps. Thus, these stresses are time dependent. However, given these variables, an attempt has been made to consider very simple ice shapes for various loads and approximate the shear stresses at the interface between the impact ice and air foil surfaces. Tensile stresses at the interface were *not* considered.

### 3.7.1 Shear Stresses in a Rotating Airfoil [10,11]

For this case, the shear stress varies linearly from the center of rotation. The maximum value occurs at the blade tip and can be approximated as follows:

$$\tau = \rho \omega^2 Rh$$

where

$\rho$ = ice density
$\omega$ = angular speed
R = radial location
h = ice thickness

For a uniform ice layer, there are no normal stresses from rotary inertia.

### 3.7.2 Aerodynamic Pressure Loading [14,15]

For the case considered, the Bragg ice shape, the peak shear stress is approximately equal to the peak pressure acting on the impact ice shape. For one case, the shear stress exceeds the peak pressure by 30%. Thus, with the limitations implied, the shear stress can be estimated by the equation below.

$$\tau \approx 1.3\ p$$

where p is the peak pressure acting on the ice.

### 3.7.3 Ice Shear Stresses and Normal Stresses from Shear Forces on an Airfoil with Impact Ice [19]

At a cross section of a airfoil with a shear force, V, acting on the section the interface shear stress can be approximated by the following equation.

$$\tau = Vt_i y_i E_i / E_s I_t$$

where

V = shear force on section
$E_i/E_s$ = ratio of the ice modulus to the substrate modulus
$t_i$ = ice thickness
$y_i$ = distance to the shear stress location from the section CG
$I_t$ = total section modulus

If $\sigma_s$ is the normal (bending) stress in the airfoil, the normal stress in the ice, $\sigma_i$, is

$$\sigma_i = E_i/E_s \sigma_s$$

### 3.7.4 Ice Shear Stresses and Normal Stresses from Twisting of a Airfoil with Impact Ice [19]

If there is no warping of an airfoil from twisting, the ice shear stresses are zero. A circular section will not warp. However, noncircular sections will warp and, therefore, will develop ice shear stresses. However there is no simple approximation known to the authors to determine these stresses without modeling the particular section being considered.

Normal stresses will be zero in a prismatic section as long as the warping of the section is not constrained. Thus normal stresses from twisting depend on the support at the base of the section. If the section is free to distort axially at the support, the axial stresses in the section will be zero.

## 4.0 SUGGESTIONS FOR FUTURE RESEARCH

The main goals of this research project was to develop structural analyses of the shedding of impact ices from aircraft structures, airfoils and rotating blades. To accomplish these objectives, the mechanical properties of impact ice must be known and input to structural analyses. Analytical methods, based on finite element methods, must be developed and compared to measurement of impact ice shedding.

One of the critical needs of the area of deicing is the certification of helicopters for all weather flying. At present most helicopters are not certified to fly in icing conditions. For this reason, there was significant a significant effort made toward the understanding of stresses and deicing of impact ices accreted onto rotating airfoils. Current designs of deicing systems for most components of large commercial jets are adequate though the systems not energy efficient. However, there are some problem area at the engine inlets of gas turbines that need additional work.

One of the most significant needs for research in the area of structural analysis of impact ice on aircraft structures is for carefully run deicing experiments that can be compared to deicing analyses. Without this type of data, analyses that are conducted may be interesting but the accuracy is unknown. In this grant, use was made of available data but tests were not designed for comparative purposes.

There is also a need for additional tensile test data [20]. Preliminary results indicate that the tensile modulus of ice may vary with impact ice conditions. The properties of glaze ice approach those of natural ice. However, the modulus of rime ice may be much lower. Additional tensile data is needed. Two attempts were made in this contract to obtain data of this type but additional work remains to be done. It is suggested that impact ice specimens collected from the IRT be tensile tested in a cold room after collection and shaped to size if necessary.

The objectives of these proposed measurements is to determine the elastic modulus of impact ice from glaze to rime and to measure the tensile strength. In testing of this type, the fact that ice creeps must be factored into the test planning and procedures.

The work of Hawkes and Mellor [22] indicate a substantial differences between the tensile and compressive moduli and strength of natural ice. This difference has not be measured for impact ices. These data are needed.

There has be some work done on the fracture mechanics on natural ice by Hawkes and Mellor [22] and others [20]. This type of work should be extended to impact ices.

Additional detailed finite element analyses of real three dimensional ice shapes on both rotating and fixed airfoils should be conducted on experiments where the results of the finite element analyses can be correlated with deicing measurements. As seen in Section 3.5, stresses at the interface between the impact ice and airfoil are extremely complex. Thus it may not be possible to develop a simple equations to characterize the interface stresses except for ideal conditions.

## 5.0 ACKNOWLEDGEMENTS

The authors wish to acknowledge the contributions of the many graduate and undergraduate students that worked on this grant: namely Jeffrey Halter, Kazuyoshi Suzuki, Ateen Khatkhate, X. T. Xian, Denise Deem, R. Raju, Vaja Ananthaswamy and also to Caroline Kellackey who wrote the first draft of this final report.

The authors are also indebted to the B. F. Goodrich Company for their financial support, to the Boeing Aircraft Company for providing experimental data on the EIDI deicing system, to the computer center at the University of Akron, to the Structural Analysis and Research Corporation for providing the COSMOS/M finite element package and, finally, to the NASA Lewis Research Center for their financial support, the use of their experimental facilities and the many helpful suggestions of our contract monitors.

## 6.0 PUBLICATIONS

[1] Scavuzzo, R.J. and M.L. Chu, "Structural Properties of Impact Ices," AIAA Paper 86-0549, January 1986.

[2] Chu, M.L., R.J. Scavuzzo, and W.V. Olsen, "Measurement of Adhesive Shear Strength of Impact Ice in and Icing Wind Tunnel," Proceedings Third International Workshop on the Atmospheric Icing of Structures, Vancouver, B.C., May 1986.

[3] Scavuzzo, R.J., M.L. Chu, and P.C. Lam, "Development of a Composite Technique in the Determination of the Tensile Strength of Impact Ices," Proceedings Third International Workshop on the Atmospheric Icing of Structures, Vancouver, B.C., May 1986.

[4] Scavuzzo, R.J., M.L. Chu, and W.V. Olsen, NASA Grant (NAG3-479) Report on the "Structural Properties of Impact Ices Accreted on Aircraft Structures." NASA CR 179580, NASA LRC, 1987.

[5] Khatkhate, A.A., R.J. Scavuzzo, and M.L. Chu, "A Finite Element Study of the EIDI System," AIAA Paper 88-0022, January 1988.

[6] Scavuzzo, R.J., M.L. Chu, and C.K. Brinkmanis, "Adhesive Peal Strength of Artificial Ice," Proceedings of the 4th International Conference on Atmospheric Icing of Structures, September 5-7, 1988, Paris, France.

[7] Chu, M.L., X.T. Xian, and R.J. Scavuzzo, "Combined Finite Element-Experimental Technique," Proceedings of the 4th International Conference on Atmospheric Icing of Structures, September 5-7, 1988, Paris, France.

[8] Xian, X.T., M.L. Chu, Scavuzzo, R.J. and T.S. Srivatsan, "An Experimental Evaluation of the Tensile Strength of Impact Ice,"Journal of Material Science Letters, 8, 1989, pp. 1205-1208.

[9] Scavuzzo, R.J., M.L. Chu, E.J. Woods, R. Raju, and A.A. Khatkhate, "Finite Element Studies of the EIDI System Using Force Inputs," AIAA Paper 89-0868, January 1989.

[10] Scavuzzo, R.J., M. L. Chu, and C.J. Kellackey, "Impact Ice Stresses in Rotating Airfoils," AIAA Paper 90-0198, January 1990.

[11] Scavuzzo, R.J., M.L. Chu, and C.J. Kellackey, "Impact Ice Stresses in Rotating Airfoils," Journal of Aircraft, Vol 29, 11, Nov 1991.

[12] Scavuzzo, R.J., M.L. Chu, E.J. Woods, R. Raju, and A.A. Khatkhate, "Finite Element Studies of the EIDI System," Journal of Aircraft. Vol. 27, No. 9, p 757-62, September 1990.

[13] Chu, M.L. and R.J. Scavuzzo, "Adhesive Strength of Impact Ice," AIAA Journal, Vol 29, No. 11, Nov. 1991, pp. 1921-27.

[14] Scavuzzo, R.J., M.L. Chu and V. Ananthaswamy, "Influence of Aerodynamic Forces in Ice Shedding" AIAA Paper 90-0198, January 1990.

[15] Scavuzzo, R.J., M.L. Chu and V. Ananthaswamy, "Influence of Aerodynamic Forces in Ice Shedding," Journal of Aircraft, Vol 31, No 3 June 1994, pp. 526-30.

[16] Kellackey, C.J., M.L. Chu, and R.J. Scavuzzo, "Statistical Structural Analysis of Rotor Impact Ice Shedding," AIAA Paper 91-0663, January 1991.

[17] Scavuzzo, R.J., M.L. Chu, and C.J. Kellackey, "Tensile Properties of Impact Ices," AIAA Paper 92-0883, January 1992.

[18] Chu, M.L., R.J. Scavuzzo, T.S. Srivatsan, "A Combined Analytical Experimental Tensile Test Technique for Brittle Materials," SEM, Experimental Mechanics, Vol. 46,No. 1,Jan./Feb. 1992, pp. 46-50.

[19] Scavuzzo, R.J., M.L. Chu, and C.J. Kellackey, "Impact Ice Interface Shear Stresses Caused be Blade Bending and Twisting" AIAA Paper 93-0030, January 1993.

[20] Reich, A., R. J. Scavuzzo, and M. L. Chu, "Survey of Mechanical Properties of Impact Ice," AIAA 94-0712, January 1994.

[21] Kellackey, C. J., The Probability of Ice Shedding from a Rotating Airfoil, Master of Science Thesis, The University of Akron, Akron, OH May 1990.

[22] Hawkes, I. and M. Mellor, "Deformation and Fracture of Ice Under Uniaxial Stress," Journal of Glaciology, Vol 11, No. 6, 1972, pp. 103-33.

[23] Jellinek, H.H.G. ,"The Influence of Imperfections on the Strength of Ice", Jr. of Applied Physics, Vol. 27 No.10, 1958, pp 1198-1209.

[24] Druez, J., Laforte, L., Trembley, C., "Experimental Results on the Tensile Strength of Atmospheric Ice", Eighth International Conference on Offshore Mechanics and Arctic Engineering, The Hague, March, 1989, pp. 405-10.

[25] Druez, J., Cloutier, J., Claveau, L., "Etude Comparative de la Resistance a la Traction et a la Compression de la Glace Atmospherique", Jr. de Physique Colloque C1, Supplément au nº 3, Tome 48, mars 1987, pp C1-337 to C1- 343.

[26] Druez, J., Claveau, L., Trembley, C., "La Mesure de la Resistance en Traction de la Glace Atmospherique", Eleventh Canadian Congress of Applied Mechanics, Univ. of Alberta, May 1987

[27] Reich, A.D., "Comparison of Rime and Glaze Deformation and Failure Properties", AIAA Paper 91-0446, Jan. 1991.

[28] Reich, A.D., "Ice Property/Structure Variations Across the Glaze/Rime Transition", AIAA Paper 92-0296, Jan. 1992.
[29] Itagaki, K.I., "Mechanical Ice Release Processes: Self Shedding Ice from High Speed Rotors," CRREL Report 83-26, October 1983.

# REPORT DOCUMENTATION PAGE

*Form Approved*
*OMB No. 0704-0188*



| 1. AGENCY USE ONLY (*Leave blank*) | 2. REPORT DATE | 3. REPORT TYPE AND DATES COVERED |
|---|---|---|
| | April 1996 | Final Contractor Report |

**4. TITLE AND SUBTITLE**

Structural Analysis and Properties of Impact Ices Accreted on Aircraft Structures

**5. FUNDING NUMBERS**

WU-505-68-10
G-NAG3-479

**6. AUTHOR(S)**

R.J. Scavuzzo, M.L. Chu, and C.J. Kellackey

**7. PERFORMING ORGANIZATION NAME(S) AND ADDRESS(ES)**

University of Akron
Akron, Ohio 44325-0001

**8. PERFORMING ORGANIZATION REPORT NUMBER**

E-10195

**9. SPONSORING/MONITORING AGENCY NAME(S) AND ADDRESS(ES)**

National Aeronautics and Space Administration
Lewis Research Center
Cleveland, Ohio 44135-3191

**10. SPONSORING/MONITORING AGENCY REPORT NUMBER**

NASA CR-198473

**11. SUPPLEMENTARY NOTES**

Project Manager, David N. Anderson, Propulsion Systems Division, NASA Lewis Research Center, organization code 2720, (216) 433-3585.

**12a. DISTRIBUTION/AVAILABILITY STATEMENT**

Unclassified - Unlimited
Subject Categories 03 and 27

This publication is available from the NASA Center for AeroSpace Information, (301) 621-0390.

**12b. DISTRIBUTION CODE**

**13. ABSTRACT** (*Maximum 200 words*)

This final contractor report presents a summary of work done on the experimental measurements of the mechanical properties of impact ices and analytical studies of ice stresses and mechanical deicing systems. Experimental work on the adhesive shear strength, the peel strength, the bending strength and tensile strength of impact ices. The major analytical studies that were completed are as follows: (1) Ice shedding by the EIDI system, (2) Impact Ice stresses in rotating airfoils, (3) Aerodynamic forces in ice shedding, (4) Interface shear stresses from bending and twisting, and (5) Statistical structural analysis of ice shedding from rotating airfoils. In this report, results and data from each experimental and analytical study are summarized. A total of twenty (20) technical papers and one MS Thesis were written and/or presented from the work done in this project.

**14. SUBJECT TERMS**

Experimental measurements; Mechanical properties; Impact ices; Ice stresses; Mechanical deicing systems

**15. NUMBER OF PAGES**

44

**16. PRICE CODE**

A03

| 17. SECURITY CLASSIFICATION OF REPORT | 18. SECURITY CLASSIFICATION OF THIS PAGE | 19. SECURITY CLASSIFICATION OF ABSTRACT | 20. LIMITATION OF ABSTRACT |
|---|---|---|---|
| Unclassified | Unclassified | Unclassified | |

National Aeronautics and
Space Administration

**Lewis Research Center**
21000 Brookpark Rd.
Cleveland, OH 44135-3191